Improvement of pyranose 2-oxidase from *Trametes multicolor* regarding the conversion of D-galactose by rational protein design and directed evolution

Katrin Radakovits, Oliver Spadiut, Dietmar Haltrich

Betreuer

Department for Food Science and Technology, BOKU-University of Natural Resources and Applied Life Sciences, A-1190 Vienna, Austria

Dipl.-Arb., 2008

PART I

Improvement of pyranose 2-oxidase from *Trametes multicolor* regarding the conversion of D-galactose by rational protein design

Katrin Radakovits[1], Oliver Spadiut[1], Dietmar Haltrich[1]

[1] Department of Food Sciences and Technology, BOKU-University of Natural Resources and Applied Life Sciences, A-1190 Vienna, Austria

Abstract

Pyranose 2-oxidase (P2Ox) is a fungal enzyme which participates in lignin degrading processes of wood rot fungi. P2Ox oxidizes several aldopyranoses at the C2 to the corresponding ketoaldoses. Recently P2Ox gained increased attention as versatile biocatalyst in food technology, for example for the production of non-cariogenic, low-caloric D-tagatose. The aim of this work was to elucidate the effects of various mutations in the active site of P2Ox on its catalytic activity and to improve the catalytic efficiency of the P2Ox in regard of its D-galactose conversion. This was approached by altering the enzyme with the method of site-directed mutagenesis.

In order to enhance the catalytic activity of pyranose 2 oxidase for the poor substrate D-galactose site directed mutagenesis introducing changes at position V546, E542 and T169 located in the active site was performed. Mutant V546C was already known to have a positive effect on the K_M value of pyranose 2-oxidase for D-galactose substrate. Mutant E542K was known to have a positive effect on the thermostability of the mutant enzyme. The resulting mutational variant V546C/E542K/T169G showed with the substrate D-glucose a slightly decreased K_M value and a very low turnover number compared to the wildtype using oxygen or 1,4-benzoquinone as electron acceptor. Using D-galactose as substrate and oxygen as electron acceptor the K_M value decreased significantly for 40-times, but the mutant enzyme showed also a 10-time decreased turnover number, resulting in a 3-times higher catalytic efficiency compared to the wildtype enzyme. While using D-galactose as substrate and 1,4-benzoquinone as electron acceptor the K_M value decreased for 2.5-times and the reaction speed was accelerated for 10-times.

The mutations V546C/E542K/T169G resulted in a mutant enzyme with a 25-times better catalytic efficiency in contrast to the wildtype enzyme using D-galactose as substrate and 1,4-benzoquinone as electron acceptor.

Introduction

Pyranose 2-oxidase (P2Ox; pyranose 2-oxidoreductase; glucose 2-oxidase; EC 1.1.3.10) is a FAD dependent enzyme in wood degrading basidiomycetes and takes part in lignin degrading processes (15). P2Ox is localized preferentially in the hyphal periplasmic space (4) of lignocellulolytic fungi. Only during autolysis P2Ox is located extracellularly and is associated with fungal cell walls or with extracellular slime (2, 3). The enzyme has a proposed role in lignocellulose degradation. P2Ox oxidizes aldopyranoses at position C2 to the corresponding ketoaldoses. The hydrogen peroxide (H_2O_2), which is produced during the reaction, is the essential co-substrate for lignin peroxidase and manganese peroxidase. P2Ox was purified and characterized from a number of microorganisms, like *Phanerochaete chrysosporium, Phlebiopsis gigantean, Pleurotus ostreatus, Polyporus obtusus* and *Trametes multicolor* (6, 11, 14). In this study P2Ox from *Trametes multicolor* was used.

Pyranose 2-oxidase is a large, homotetrameric flavoprotein with a molecular weight of approximately 270 kDa and consists of four identical 68 kDa subunits (12). A flavin adenine dinucleotid (FAD) acts as a cofactor and is covalently bound to each of the four subunits at the N3 of the His167 residue via an 8α-methylic group (8).

P2Ox catalyzes the regioselective oxidation of several aldopyranoses at the C2 position by molecular oxygen, forming the corresponding 2-ketoaldoses and H_2O_2 (4, 7). During the reductive half-reaction, the sugar is oxidized to the corresponding ketosugar and the co-factor FAD is reduced to $FADH_2$ (see equation a).

The following oxidative half-reaction involves the reduction of O_2 to H_2O_2 and the regeneration of the co-factor (see equation b).

D-glucose + FAD → 2-keto-D-glucose + $FADH_2$ (a)

$FADH_2 + O_2 \rightarrow FAD + H_2O_2$ (b)

Regarding the catalytic activity of *Tm*P2O the monosaccharide D-glucose is the preferred substrate. A range of C6 sugars, such as D-galactose, can also be utilized by P2Ox. D-galactose performs poorly as substrate for *T. multicolor* P2Ox with only 5.2% relative activity compared to D-glucose (12).
P2Ox can be used as key biocatalyst in several biotechnological applications. The oxidized 2-keto-sugars obtained from D-galactose and D-glucose can be reduced catalytically or enzymatically at position C1 to obtain high yields of virtually pure D-tagatose and D-fructose, respectively. The ketose sugar D-tagatose has a significant potential as a non-cariogenic, low caloric sweetener used in food applications.
Applications of P2Ox in the field of bioprocess monitoring, clinical chemistry analytics and synthetic carbohydrate chemistry have already been reviewed by Giffhorn (7).
For effective biotechnological application P2Ox has to be changed in respect to substrate specificity and improved in catalytic efficiency. In this study we improved the catalytic efficiency of P2Ox for the poor substrate D-galactose through site-directed mutagenesis.

Material and Methods

Bacteria strains, media and plasmids
All chemicals used were purchased from SIGMA and were of the purest grade available. Active P2Ox and P2Ox mutants were expressed in the *E. coli* strain BL21 DE3 (Invitrogen). TB_{amp} medium (yeast extract 24 $g \cdot L^{-1}$, peptone from casein 12 $g \cdot L^{-1}$, glycerol 4 $mL \cdot L^{-1}$; KH_2PO_4 buffer 1 M, pH 7.5) was used to grow *E. coli* cells for protein expression, ampicillin (100 $mg \cdot L^{-1}$) was added for selection.
The plasmid pHL2 has been described by Kujawa et al. (10). It expresses the His tagged wildtype pyranose 2-oxidase gene regulated by the T7 promoter. The vector pHL2 was derived from the expression vector $pET21d^+$.

The plasmid carrying the T169G mutation is a variant of pHL2. The mutant T169G was described by Spadiut et al. (13).
The plasmid carrying the V546C/E542K mutation is another variant of pHL2. The variant V546C/E542K was described by Spadiut et al. (14) for P2Ox derived from *Trametes multicolor.*

Mutant construction

Mutant V546C/E542K/T169G was constructed by using the plasmid carrying the V546C/E542K mutation as template for site-directed mutagenesis to introduce the mutation T169G. For introducing the mutation T169G the primers T169G_fwd (5´-gtcgtcggaggcatgtctacgcactggggatgcgccacacc-3´) and H167A_rev (5´-cgtagacatgcctccgacgacg-3´) were used.
The PCR mixture contained Phusion Mastermix (according producer), 0.5 µg template (V546C/E542K) and 10 mM of each Primer.
The PCR conditions were 98°C for 30 sec, 30 cycles of 98°C for 10 sec, 55°C for 20 sec, and 72°C for 4 min and 7 min at 72°C for final incubation.
The PCR products were digested by 20 Units DpnI (Fermentas) to digest methylated, unmutated template DNA. Remaining PCR products were purified using Wizard®SV Gel & PCR Clean-Up System (Promega). 7 µl of the purified PCR product were transformed into electro-competent BL21 DE3 cells. To confirm the presence of the mutation and the absence of other mutations, plasmidic DNA of several mutants was extracted and used for DNA sequencing of the P2Ox encoding gene. The primers used were T7prom_fwd (5´- AATAC GACTCACTATAGGG –3´) and T7term_rev (5´-GCTAGTTATTGCTCAGCGG -3´). DNA sequencing was done as a commercial service by VBC-Biotech Services GmbH (Vienna).

Biomass production

BL21 DE3 transformants were grown in TB_{amp} media in baffled shaking flasks (37°C, 160 rpm) to an OD_{600} of ~ 0.5. Protein expression was then induced by adding D-lactose to a final concentration of 0.5% (w/v) and cultures were further grown at 25°C and 140 rpm. After 20 hours the biomass was harvested by centrifugation (6000 rpm, 30 min), diluted in the fourfold amount of KH_2PO_4 buffer (50 mM KPP, 20 mM imidazole, 0.5 mM NaCl, pH 6.5) containing 0.1% PMSF (phenylmethylsulfonylfluorid) and lysed twice using the APV-2000 pressure

homogenizer (Unna, Germany). The cells were separated from the crude extract by ultracentrifugation (30000 rpm, 30 min, and 4°C) with a Beckman L70 Ultracentrifuge.

Protein purification

The supernatant was applied onto an IMAC (immobilized metal ion affinity chromatography) column. Utilising the binding effect of the pHL2 coded C-terminal His_6 groups with a Ni-sepharose gel, a His trap column (Amersham Biosciences) was used to purify the P2Ox mutants.

P2Ox was eluted with an elution buffer containing 50 mM KPP, 1 M **i**midazole, 0.5 mM NaCl (pH 6.5) with an imidazole gradient (0-100%, 60 mL, 3 $mL \cdot min^{-1}$) from 20 mM to 1 M.

The purified enzyme was washed with KH_2PO_4 buffer (50 mM KPP)**,** desalted and concentrated using Amicon® Ultra Centrifugal Filter Device (Millipore) with a cut off of 10 kDa to a final protein concentration of 5 - 10 $mg \cdot mL^{-1}$.

The purified enzymes for the conversion experiment were desalted in a dialyse hose hanging in 22 L KPP buffer (5 mM).

Protein concentration and activity measurements

Protein concentrations were determined by the Bradford assay (1). Bovine serum albumine (BSA) was used as standard.

The standard enzyme activities were measured with the chromogenic ABTS assay (5). 10 µl of the diluted enzyme were added to 990 µl of the reaction solution tempered to 30°C. The reaction solution contained 523.8 µg ABTS [2,2´-azinobis(3)-ethylbenzthiazolinesulfonic acid], 142 Units horseradish peroxidase, KH_2PO_4 buffer (50 mM, pH 6.5) and either D-glucose (0.1-50 mM) or D-galactose (0.1-200 mM). The absorbance change at a wavelength of 420 nm was measured for 180 seconds. One unit P2Ox was defined as the amount of enzyme needed to oxidize 2 µmol of ABTS per minute. The chromophore ε_{420} used was 42.3 $mM^{-1}cm^{-1}$.

Additionally, the catalytic constants for 1,4-benzoquinone (1,4-BQ) as electron acceptor were determined by adding 10 µl of diluted enzyme to 990 µl assay buffer containing either D-glucose or D-galactose (100 mM), KH_2PO buffer (50 mM, pH 6.5) and 1,4-benzoquinone in varying concentrations (0.01-1.0 mM). The absorbance change at 290 nm was recorded at 30°C for 180 seconds. The chromophore ε_{290} used was 2.24 $mM^{-1}cm^{-1}$.

Thermostability

The thermostability was determined by exposing the enzyme to temperatures of either 60°C or 70°C for varying time intervals. The exposing time intervals for 60°C were 0 min (no temperature exposure), 0.5 min, 1 min, 2 min, 5 min, 10 min, 30 min, 60 min, 120 min, 160 min, 600 min and for 70°C exposure temperature 0 min (no temperature treatment), 0.167 min, 0.5 min sec, 1 min, 5 min, 10 min, 20 min, 30 min, 60 min, 120 min, 180 min.

After heat treatment the enzymes were cooled on ice and the remaining activity was measured by an ABTS enzymatic activity assay with D-galactose as substrate (200 mM) and oxygen as electron acceptor.

Conversion

The conversion experiment was set up in six seperate reactors. The reactors were filled with 225 ml sodiumcitrate-puffer (125 mM, pH 5.0) and 100000 Units catalase were added. The catalase was applied in excess to assure an effectual amount in the conversion broth. The reactors with 1,4-benzoquinone as electron acceptor, 3 mM 1,4-benzoquinone and 100 Units laccase were added. The laccase was applied in the three-fold amount of the applied enzyme to exclude limitations because of a missing regeneration of the 1,4-benzoquinone. The purpose of the laccase was the regeneration of the 1,4-benzoquinone. During the conversion, every three hours 100000 Units catalase were replenished.

In the six reactors of the conversion experiment dominated following conditions and the reaction mixture was composed of the following components:

Table 1: Components and conditions of each reactor of the conversion experiment

reactor	1	2	3	4	5	6
enzyme	V546C/ E542K/ T169G	V546C/ E542K/ T169G	V546C/ E542K/ T169G	V546C/ E542K/ T169G	wildtype	wildtype
amount of enzyme	36.76 mg	3.68 mg	36.76 mg	3.68 mg	47.78 mg	4.78 mg
specific activity D-glucose/ D-galactose	0.02/ 0.12 $U \cdot mg^{-1}$	1.8/ 3.54 $U \cdot mg^{-1}$	0.001/ 0.02 $U \cdot mg^{-1}$	3.95/ 6.32 $U \cdot mg^{-1}$	7.81/ 0.5 $U \cdot mg^{-1}$	49.51/ 4.92 $U \cdot mg^{-1}$
temp.	30°C	30°C	50°C	50°C	50°C	50°C
electron acceptor	oxygen	1,4-BQ	oxygen	1,4-BQ	oxygen	1,4-BQ
amount of D-glucose/ D-galactose	0.16 $g \cdot L^{-1}$	4.7 $g \cdot L^{-1}$	0.27 $g \cdot L^{-1}$	8.37 $g.L^{-1}$	8.63 $g \cdot L^{-1}$	8.47 $g \cdot L^{-1}$

All components except of enzymes were filled into the reactors and tempered to the according temperatures. With the addition of the enzymes the conversion reaction of the D-sugars to the corresponding 2-keto-D-sugars was started.

After varying time intervals samples of 1 ml volume were extracted. Immediately after the extraction the samples were heated for 3 minutes to 99°C to inactivate the enzymes to prevent further conversion of the sugars.

The sugar content in the reaction broth was determined by a high pressure liquid chromatography (HPLC).

Results and Discussion

Enzyme kinetics of V546C/E542K/T169G

We tried to improve the catalytic efficiency of the P2Ox in regard of D-galactose conversion. This work deals with the combination of three mutations, T169G, V546C

and E542K, which were described in previous works by Spadiut et al. (13). In contrast to the wildtype enzyme the variant V546C/E542K shows a higher k_{cat} with D-galactose, but also a higher K_M value. In mutant V546C/E542K cysteine was introduced at position 546 instead of valine. This amino acid contains a SH- and an OH-group. The SH-group may lead to polar interactions and in succession to repulsion. V546C is located in the active site, the repulsion may affect the vicinity of the subunits, resulting in more space for the substrate to enter the enzyme.

Furthermore, glutamic acid at position 542 was replaced with lysine. This mutation affects positively the thermostability of the enzyme (9). The melting temperature T_m of the wild type P2Ox of 60°C was increased because of the introduction of the mutation E542K to 74°C. This is an elevation of 14°C.

For another mutant, T169G, a dramatically decreased K_M value for D-galactose was described (13). Threonine at position 169 was replaced with glycine. Glycine is the smallest amino acid and was expected to offer more space in the active site of the enzyme. Providing more space the substrate enters more easily the active site and binds better. By combining these three mutations we obtained the variant V546C/E542K/T169G. The K_M and k_{cat} values of this mutant for both sugars and oxygen as electron acceptor were determined by an ABTS assay. Additionally the kinetic data with saturated substrates, D-glucose and D-galactose, for the alternative electron acceptor 1,4-benzoquinone were determined.

The kinetic values for D-glucose and D-galactose with oxygen as electron acceptor are shown in Table 2.

Table 2: Kinetic data of wildtype P2Ox and the variant V546/E542K/T169G with either D-glucose or D-galactose as sugar substrate and oxygen as electron acceptor (air saturation)

	D-glucose			D-galactose		
	K_M (mM)	k_{cat} (s^{-1})	k_{cat}/K_M ($mM^{-1}\ s^{-1}$)	K_M (mM)	k_{cat} (s^{-1})	k_{cat}/K_M ($mM^{-1}\ s^{-1}$)
wildtype P2Ox	0.74	17.9	24.2	7.94	2.1	0.26
V546C/E542K	1.52	82.2	53.9	24.6	6.13	0.25
V546C/E542K/T169G	0.64	0.07	0.11	0.27	0.22	0.81

Using D-glucose as substrate the mutant V546C/E542K/T169G shows a K_M value of 0.64 mM, which meant a 13% decrease compared to the wild type. The change in the amino acid sequence at position 169 improved the binding of the D-glucose just slightly. Compared to the V546C/E542K mutant the K_M value of the V546C/E542K/T169G mutant is lowered for 50%. The k_{cat} value also decreased and showed a value of 0.0724 s^{-1}, this is a 200-fold decrease compared to the wild type and an 800-fold decrease compared to the V546C/E542K mutant. The catalytic efficiency of 0.1131 $mM^{-1}s^{-1}$ was 250-fold lower compared to the wildtype and 500-times lower compared to the V546C/E542K mutant, this meant that the mutant V546C/E542K/T169G hardly converts D-glucose.

Using D-galactose as substrate the mutant V546C/E542K/T169G showed a K_M value of 0.27 mM, this is a 40-fold decrease compared to the wild type and a 120-fold decrease compared to the V546C/E542K mutant. The k_{cat} value was 0.22 s^{-1}. In comparison with the wildtype this is a 10-times and in comparison with the V546C/E542K mutant a 30-times lower value. The resulting catalytic efficiency was three-times higher than the catalytic efficiencies of the wildtype and the V546C/E542K mutant (see table 3).

The V546C/E542K/T169 mutant converts galactose three-times slower, but binds it 40-times better than the wildtype. The catalytic efficiency of the conversion of D-galactose is three-times higher compared to the wildtype, while the conversion of glucose is nearly disrupted.

Table 3: Relative catalytic efficiencies of the mutant V546C/E542K/T169G compared to the wildtype P2Ox using oxygen as electron acceptor

	relative catalytic efficiency [%]	
	D-glucose	D-galactose
wildtype P2Ox	100	100
V546C/E542K	223	95
V546C/E542K/T169G	0.5	308

The catalytic constants for the alternative electron acceptor 1,4-benzoquinone were also determined with both sugars (sugar saturation). The kinetic data are shown in Table 4.

Table 4: Kinetic data of wildtype P2Ox and the variant V546/E542K/T169G with either D-glucose or D-galactose as sugar substrate and 1,4-benzoquinone as electron acceptor (air saturation)

	D-glucose			D-galactose		
	K_M (mM)	k_{cat} (s^{-1})	k_{cat}/K_M (mM^{-1} s^{-1})	K_M (mM)	k_{cat} (s^{-1})	k_{cat}/K_M (mM^{-1} s^{-1})
wildtype P2Ox	0,4	348,77	862,65	0,25	6,61	26,3
V546C/E542K	0.37	663.73	1799.71	1.52	82.22	53.92
V546C/E542K/T169G	0,22	21.16	94,57	0,09	62,81	671,03

Using D-glucose as substrate and 1,4-benzoquinone as electron acceptor the variant V546C/E542K/T169G showed a halved K_M value of 0.22 mM in comparison with the wildtype and the V546C/E542K mutant. The turnover number was 18-fold decreased compared to the wildtype and 33-fold decreased in comparison with the V546C/E542K mutant. The resulting catalytic efficiency of 94.57 $mM^{-1}s^{-1}$ meant a 10-fold decrease regarding the wildtype and a 20-fold decrease in comparison with the V546C/E542K mutant. This means the variant V546C/E542K/T169G hardly converts glucose with 1.4-benoquinone as electron acceptor.

The K_M value for the mutant V546C/E542K/T169G, using D-galactose as substrate and 1,4-benzoquinone as electron acceptor, of 0.094 mM was 2.5-fold lower regarding to the wildtype. This means the introduction of glycine instead of threonine affects positively the binding of D-galactose using 1,4-benzoquinone as electron acceptor. The turnover number was ten-times higher compared to the wildtype. This means the substrate is converted 10-times faster by the mutant V546C/E542K/T169G than by the wild type.

Summing up, the mutant V546C/E542K/T169G hardly converts D-glucose, but is 25-times (see catalytic efficiency k_{cat}/K_M) more effective in processing D-galactose than the wild type (see Table 5).

Table 5: Relative catalytic efficiencies of the mutant V546C/E542K/T169G compared to the wildtype P2Ox using 1.4-benzoquinone as electron acceptor

	relative catalytic efficiency (%)	
	D-glucose	D-galactose
wildtype P2Ox	100	100
V546C/E542K	208.63	205.03
V546C/E542K/T169G	10.96	2551.54

Thermostability

The improved thermostability due to the introduction of the E542K mutation in pyranose 2-oxidase was described by Heckmann-Pohl et al (9). In this work we tried to retain the improved thermostability caused by the E542K mutation, despite the presence of two other mutations, V546C/T169G, which improve the affinity of the mutant enzyme to D-galactose and increase the turnover number to accelerate the reaction speed.

In Figure 1 are the thermostability profiles of the mutant V546C/E542K/T169G and wildtype enzyme at 60°C shown.

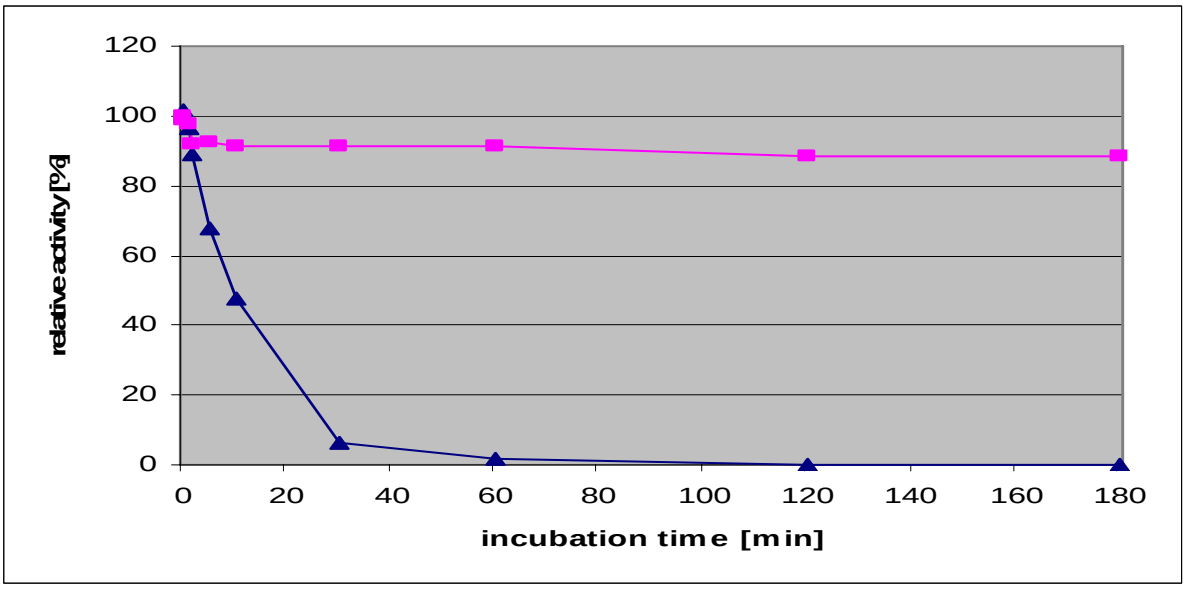

Figure 1: Thermostability profile at 60°C of the wildtype P2Ox, ▲, and the mutant enzyme, ■

The activity of the wildtype enzyme started to decrease significantly. The wildtype showed after five minutes a relative activity of 68%, after another five minutes the relative activity decreased to 48%. After one hour, the activity of the wildtype was nearly 0% in reference to the activity of the wildtype without temperature treatment. However, the mutant V546C/E542K/T169G tolerated the increased temperature for 3 hours with about 90% relative activity. After a temperature treatment of 60°C for 20 hours the V546C/E542K/T169G mutant showed a relative activity of about 23% in relation to the relative activity without temperature exposure.

The improved thermostability is also obvious at viewing the half-life time $T_{1/2}$ of the enzymes. $T_{1/2}$ of the wildtype was 8.6 minutes. By contrast, the half-life of the mutant was 693 minutes. That is an 81-fold extension (see Figures 2, 3).

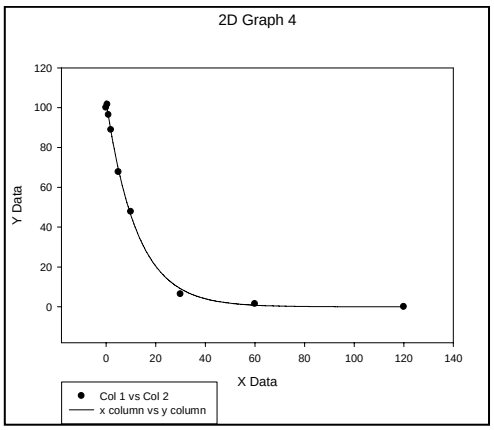

Figure 2: half-life of the wildtype enzyme at 60°C

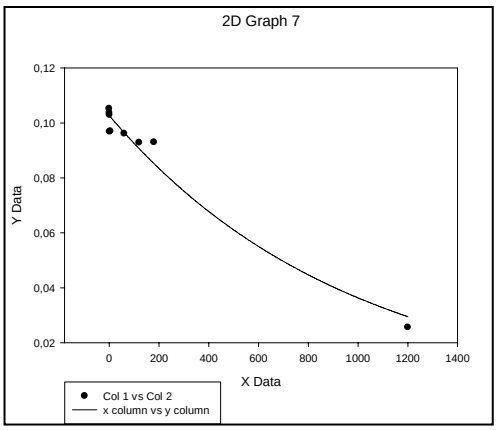

Figure 3: half-life of the mutant V546C/E542K/T169G

In Figure 4 are the thermostability profiles of the mutant V546C/E542K/T169G and the wildtype P2Ox at 60°C shown.

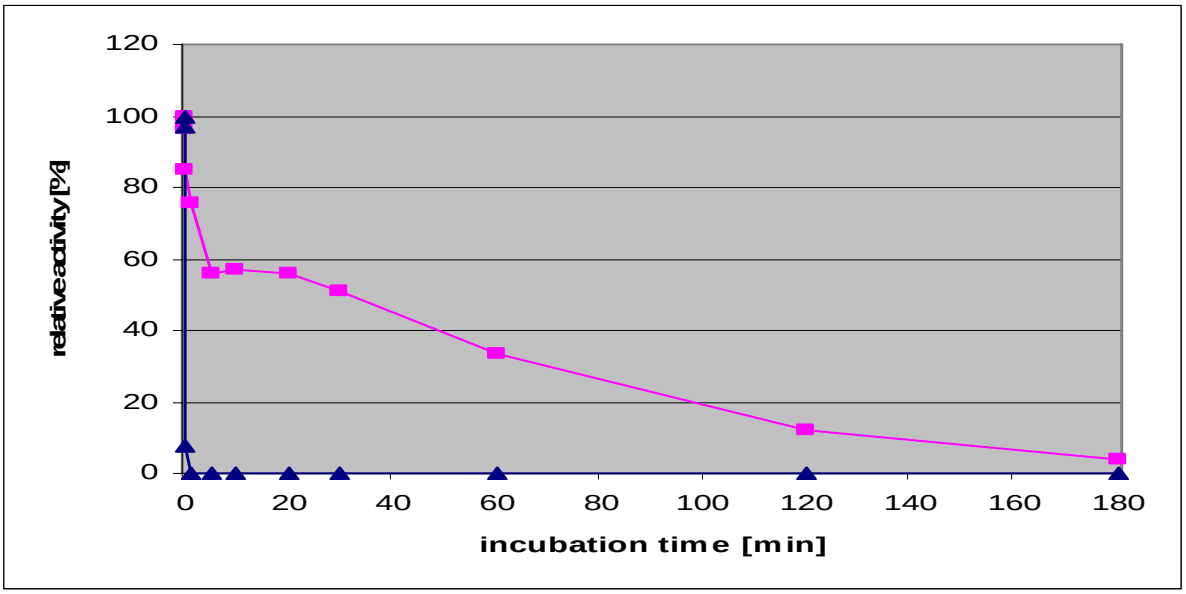

Figure 2: Thermostability profile at 70°C of the wildtype P2Ox, ▲, and mutant enzyme, ■

At 70°C the wildtype´s activity started to decrease after a few seconds and reached the zero point after one minute. The half-life was just 0.13 minutes. In contrast, the mutant V546C/E542K/T169G endured the high temperature for three hours. The activity decrease also started after a few seconds, but it was a more moderate progress. After 30 minutes the mutants still showed a relative activity of 50% and after 60 min a relative activity of 30%. After three hours the relative activity decreased to 4% in relation to the starting activity without temperature treatment. The half-life was 37.5 minutes, which means a 278-fold increase (see figures 5, 6).

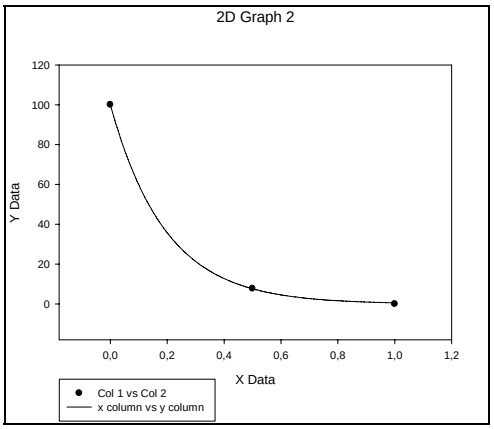

Figure 3: half-life at 70°C of the wildtype enzyme

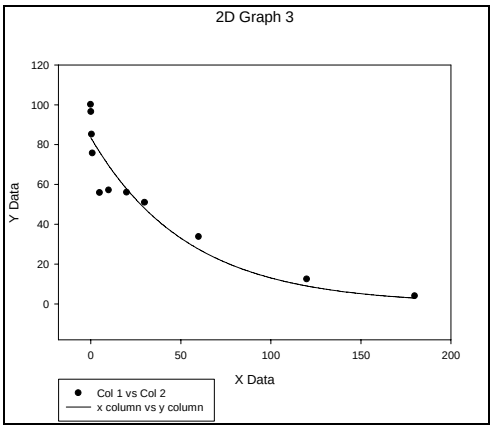

Figure 4: half-life at 70°C of V546C/E542K/T169G

These two experiments demonstrate the positive effect of the E542K mutation on the thermostability of pyranose 2-oxidase. The position of the mutation is located in the active site of the enzyme. The exchange of the glutamic acid with lysine raised due to the longer carbon chain the number of the hydrogen and so the number of additional hydrogen bonds.

Conversion results

In a conversion experiment the ability of the wildtype enzyme and the mutant V546C/E452K/T169G to convert D-glucose and D-galactose to the according 2-keto-D-sugar at certain temperatures was determined.

The conversion of D-glucose and D-galactose to the corresponding 2-keto-D-sugar at 30°C with oxygen as electron acceptor produced the following results (see figures 7 and 8).

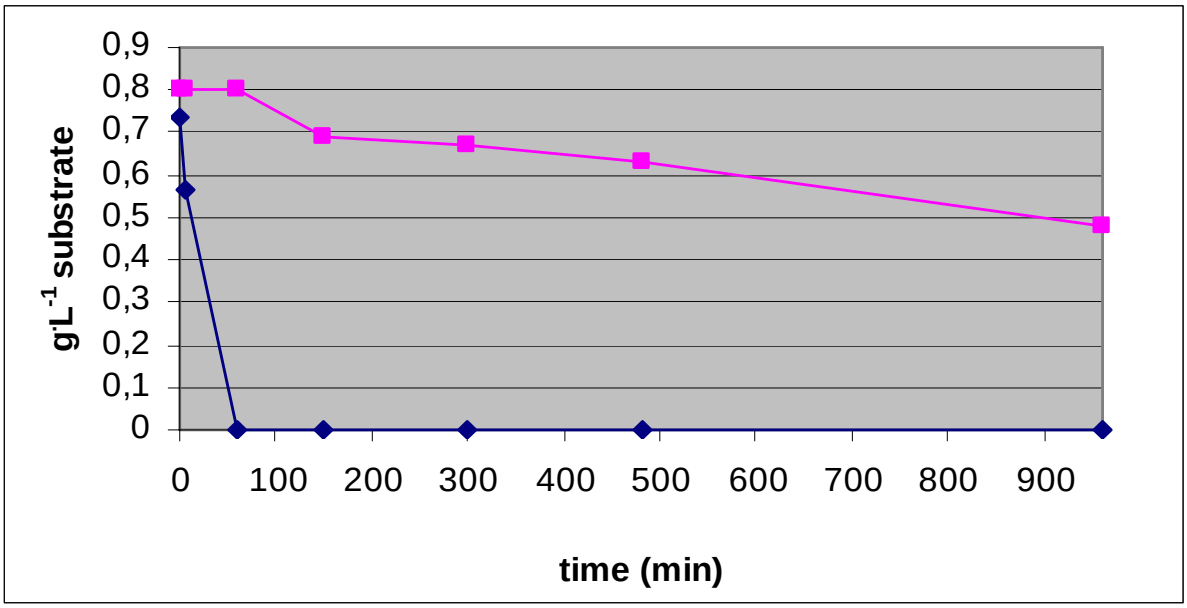

Figure 5: Conversion of the substrates D-glucose, ♦, and D-galactose, ■, at 30°C and O_2 as electron acceptor using the wildtype enzyme

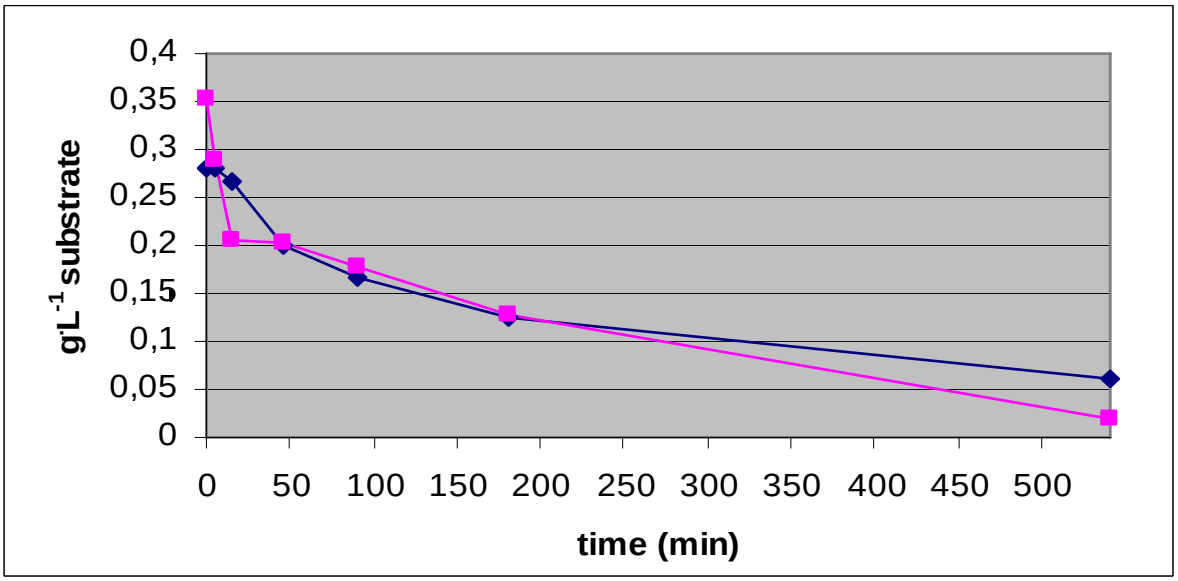

Figure 6: Conversion of the substrates D-glucose, ▲, and D-galactose, ■, at 30°C and O_2 as electron acceptor using the mutant V546C/E542K/T169G

The wildtype enzyme did not start to convert D-galactose until D-glucose was gone. D-glucose was completely converted at the measurement after 60 minutes, then the wildtype enzyme started to oxidize D-galactose, but also after a reaction time of

16 hours still 60% of the initial concentration of D-galactose were left. The conversion rates of 2 $g \cdot L^{-1} \cdot h^{-1}$ for D-glucose and 0.021 $g \cdot L^{-1} \cdot h^{-1}$ for D-galactose reflect the higher affinity of the wildtype enzyme to D-glucose.

The V546C/E542K/T169G mutant started to convert both sugars simultaneously. Both D-glucose and D-galactose was oxidized by the mutant enzyme with almost the same conversion rate: 0.05 $g \cdot L^{-1} \cdot h^{-1}$ for D-glucose and 0.056 $g \cdot L^{-1} \cdot h^{-1}$ for D-galactose. After a conversion time of 20 hours 17% of D-glucose were left and D-galactose was completely, expect less than 1%, converted into the corresponding 2-keto-D-sugar. This meant the introduction of the mutations V546C/E542K/T169G affects the substrate affinity of the mutant enzyme in favour for D-galactose.

The conversion rates of the wildtype enzyme and the mutant enzyme at 30°C and 1,4-benzoquinone as electron acceptor were also determined (see tables 9 and 10).

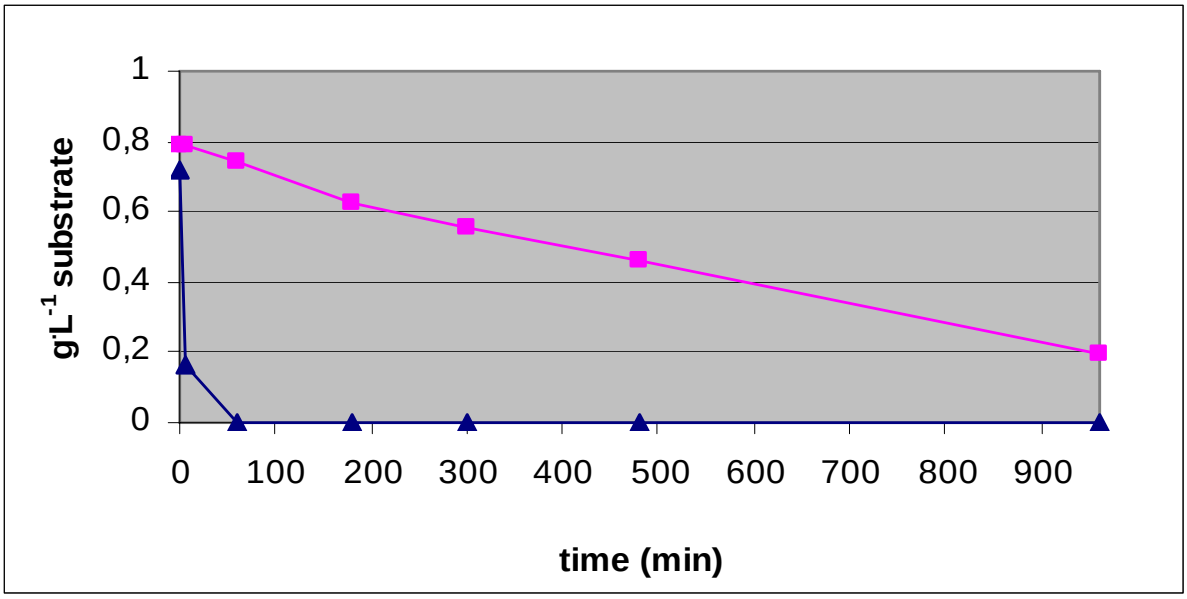

Figure 7: Conversion of the substrates D-glucose, ▲, and D-galactose, ■, at 30°C and 1,4-benzoquinone as electron acceptor using the wildtype enzyme

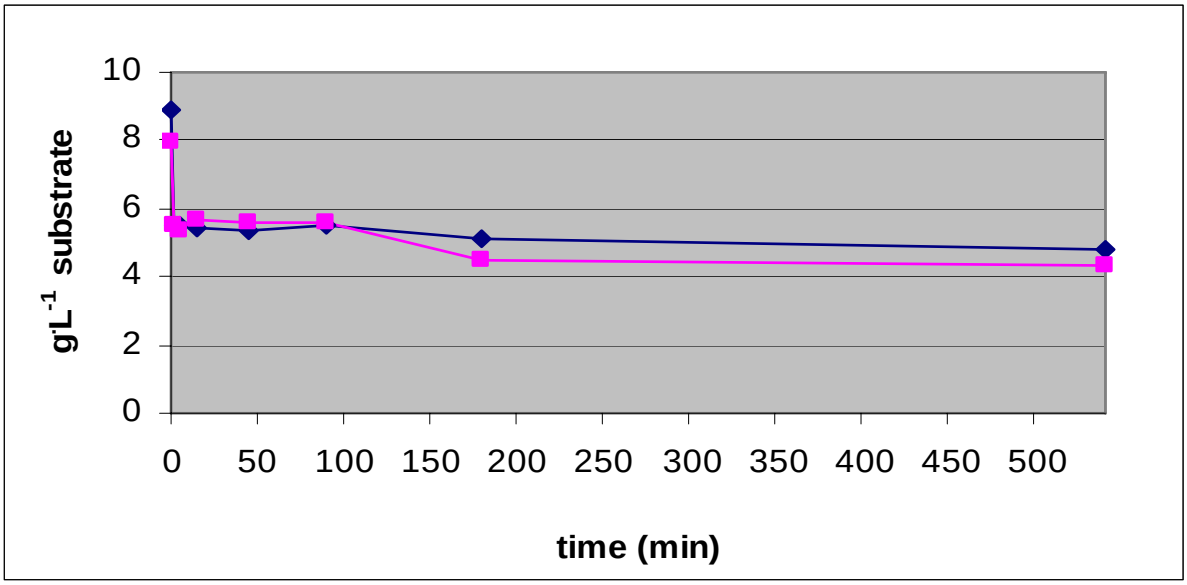

Figure 8: Conversion of the substrates D-glucose, ▲, and D-galactose, ■, at 30°C and 1,4-benzoquinone as electron acceptor using the mutant V546C/E542K/T169G

The situation with the wildtype enzyme and 1,4-benzoquinone was almost the same like the conversion experiment with O_2 as electron acceptor. The wildtype enzyme started to oxidize D-glucose, while D-galactose remained in its initial condition. Not until D-glucose was completely consumed after 60 minutes the enzyme started to oxidize D-galactose to 2-keto-D-galactose. After a reaction time of 16 hour 25% of the initial D-galactose concentration were left in the reaction broth. The wildtype enzyme showed differing conversion rate of 6.67 $g \cdot L^{-1} \cdot h^{-1}$ for D-glucose and 0.038 $g \cdot L^{-1} \cdot h^{-1}$ for D-galactose. This meant D-glucose was converted 180-times faster than D-galactose. The mutant V456C/E542K/T169G started as well in this test arrangement to convert both sugars concurrently to their corresponding 2-keto-D-sugars. The conversion rates of 0.078 $g \cdot L^{-1} \cdot h^{-1}$ for D-glucose and 0.112 $g \cdot L^{-1} \cdot h^{-1}$ for D-galactose reflect the slightly higher affinity of the mutant enzyme to D-galactose. After a reaction time of 20 hour 52% of the initial concentration of D-glucose and 48% of the initial concentration of D-galactose were left. This final concentration is a result of the inactivation of the laccase after 200 min. It is apparent that the introduction of the mutation V546C/E542K/T169G changed the substrate affinity in support of D-galactose.

These conversion experiments were also performed at 50°C to show the improved thermostability of the mutant V456C/E542K/T169G in contrast to the wildtype using either 1,4-benzoquinone or oxygen as electron acceptor (see tables 11 and 12).

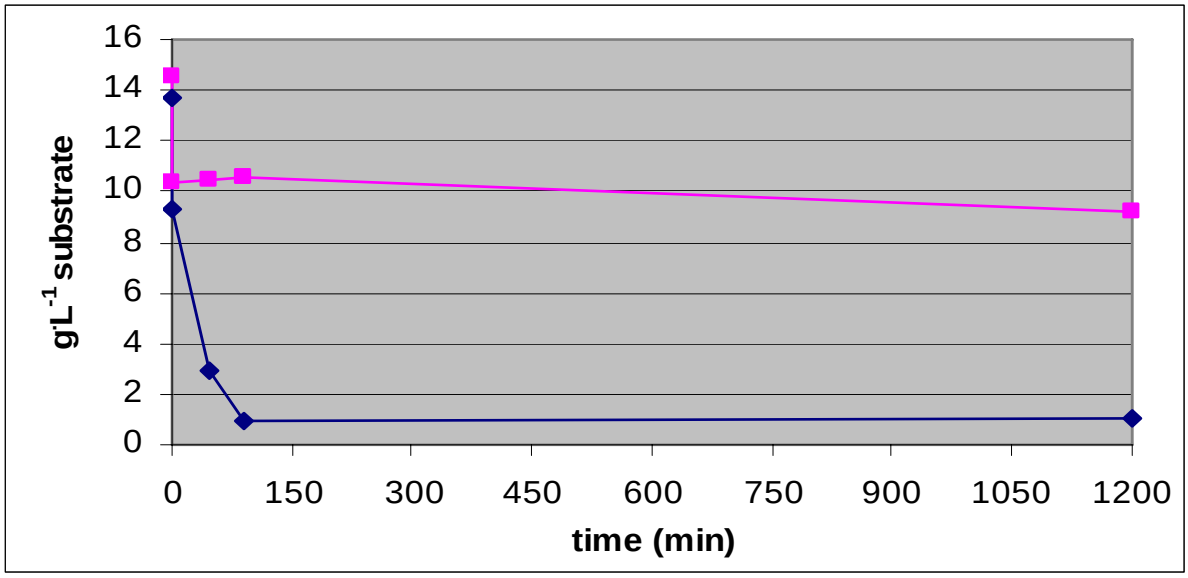

Figure 9: Conversion of the substrates D-glucose, ▲, and D-galactose, ■, at 50°C and O_2 as electron acceptor using the wildtype enzyme

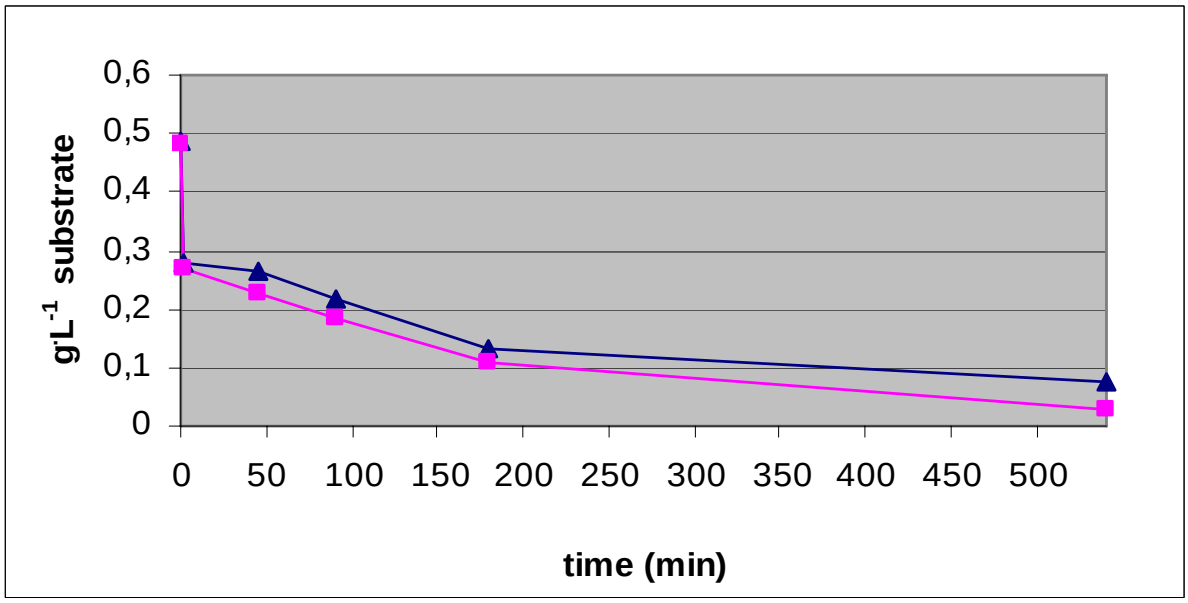

Figure 10: Conversion of the substrates D-glucose, ▲, and D-galactose, ■, at 50°C and O_2 as electron acceptor using the mutant V546C/E542K/T169G

The wildtype enzyme converted D-glucose and D-galactose into its corresponding 2-keto-D-sugar. At the end of the conversion experiment after 20 hours the concentration of the disadvantaged sugar D-galactose remained at 63% of the initial concentration. D-glucose was oxidized till a final concentration of 8% after 45 minutes. After 90 minutes the wildtype enzyme was inactivated due to the temperature of 50°C. The final D-glucose concentration remained at 1 $g \cdot L^{-1}$ because

further oxidation was not possible due to the inactivation of the wildtype enzyme. The conversion ratey of 5.67 $g \cdot L^{-1} \cdot h^{-1}$ for D-glucose and 0 $g \cdot L^{-1} \cdot h^{-1}$ for D-galactose reflect once more the higher substrate affinity of the wildtype enzyme to D-glucose.

The mutant enzyme started to oxidize both sugars simultaneously. The mutant enzyme exhibited for both D-glucose and D-galactose almost the same conversion rates as in the conversion experiment at the temperature of 30°C: 0.05 $g.L^{-1}.h^{-1}$ for D-glucose and D-galactose. This means the mutant enzyme converts the sugar despite the elevated temperature with the same rate. After a conversion time of 20 hours 11% of D-glucose were left and 1% of D-galactose was left. This meant the introduction of the mutations V546C/T169G/E542K affects the substrate affinity of the mutant enzyme in favour for D-galactose and improves the thermostability of the enzyme.

The conversion rates of the wildtype enzyme and the mutant enzyme at 50°C and 1,4-benzoquinone as electron acceptor were also determined, but delivered unevaluable results. This may result because of the thermoinstability of the laccase, which duty was to regenerate the 1,4-benzoquinone (see equations c and d).

$$BQ + e^- \rightarrow HQ \qquad (c)$$

$$HQ + \text{laccase} + O_2 \rightarrow BQ + H_2O \qquad (d)$$

Crystallography

At the KTH in Stockholm the crystal structures of the mutants H450G, F454P, Y456W, loop deletion and T169G/V546C/E542K were determined.

For the crystallization of the mutant enzymes the ´hanging drop´ method was used. The diluted enzyme solution and the crystallization buffer containing either 2-Morpholinoethanesulfonic acid Monohydrate (Mes) or Acetate were applied in a drop on a thin plate. In each well of a 24-well plate the crystallization buffer was added and covered with the thin plate, the drop hanging downwards. In the covered wells emerge a fluid-vapour balance and the crystals begin to grow.

The crystal structure was determined at the synchrotron at the Max Laboratory in Lund by Prof. Divne.

References

1 **Bradford, M. M. 1976.** A Rapid and Sensitive Method for the Quantitation of Microgram Quantities of Protein Utilizing the Principle of Protein-Dye Binding. Anal. Biochem. 72: 248-254.

2 **Daniel, G. 1994.** Use of electron microscopy for aiding our understanding of wood biodegradation. FEMS Microbiol. Rev. 13: 199-233.

3 **Daniel, G., J. Volc, E. Kubatova, and T. Nilsson. 1992.** Ultrastructural and immunocytochemical studies on the H_2O_2-producing enzyme pyranose oxidase in Phanerochaete chrysosporium grown under liquid culture conditions. Appl. Environ. Microbiol. 58: 3667-3676.

4 **Daniel, G., J. Volc, and E. Kubatova. 1994.** Pyranose oxidase, a major source of H_2O_2 during wood degradation by Phanerochaete chrysosporium, Trametes versicolor, and Oudemansiella mucida. Appl. Environ. Microbiol. 60: 2524-2532.

5 **Danneel, H.-J., Rössner, E., Zeeck, A., and Giffhorn, F. 1993.** Purification and characterization of a pyranose oxidase from the basidiomycete Peniophora gigantea and chemical analysis of its reaction products. Eur. J. Biochem. 214: 795–802.

6 **Danneel, H.-J., M. Ullrich, and F. Giffhorn. 1992.** Goal-oriented screening method for carbohydrate oxidases produced by filamentous fungi. Enzyme Microb. Technol. 14: 898-903.

7 **Griffhorn, F. 2000.** Fungal pyranose oxidases: occurrence, properties and biotechnological applications in carbohydrate chemistry. Appl. Microbiol. Biotechnol. 54: 727-740.

8 **Hallberg, B. M., C. Leitner, D. Haltrich, and C. Divne. 2004.** Crystal structure of the 270 kDa homotetrameric lignin-degrading enzyme pyranose 2 oxidase. *J. Mol. Biol.* 341: 781–796.

9 **Heckmann-Pohl D., S. Bastian, S. Altmeier, and I. Antes. 2006.** Improvement of the fungal enzyme pyranose 2-oxidase using protein engineering. *Appl. Journal of Biotechnologie, 124: 26-40.*

10 **Kujawa, M., H. Ebner, C. Leitner, B**. **Hallberg, M. Prongjit, J. Sucharitakul, R. Ludwig, U. Rudsander, C. Peterbauer, P. Chaiyen, D. Haltrich, and C. Divne. 2006.** Structural Basis for Substrate Binding and Regioselective Oxidation of Monosaccharides at C3 by Pyranose 2-Oxidase. *J. Biol. Chem.* 46: 35104-35115.

11 **Leitner, C., D. Haltrich, B. Nidetzky, H. Prillinger, and K. D. Kulbe. 1998.** Production of a novel pyranose 2-oxidase by basidiomycete *Trametes multicolor*. Appl. Biochem. Biotechnol. 70-72: 237-248.

12 **Leitner, C., J. Volc, and D. Haltrich. 2001.** Purification and characterization of pyranose oxidase from the white rot fungus *Trametes multicolor*. *Appl. Environ. Microbiol.* 67: 3636–3644.

13 **Spadiut, O., C. Leitner, T.-C. Tan, R. Ludwig, D. Divne, and D. Haltrich. 2007**. Mutations of Thr169 affect substrate specificity of pyranose 2-oxidase from Trametes multicolor. *Biocatal. Biotransfor.*; ISSN 1024-2422.

14 **Spadiut, O., I. Pisanelli, T. Maischberger, C. Salaheddin, C. Peterbauer, L. Gorton, and D. Haltrich. 2007.** Engineering of pyranose 2-oxidase: improvement for biofuel cell and food applications through semi-rational protein design. Submitted to protein science.

15 **Volc, J., N. P. Denisova, F. Nerud, and V. Musílek. 1985.** Glucose-2-oxidase activity in mycelia cultures of basidiomycetes. Folia Microbiol. 30: 141-147.

PART II

Abbreviations

ABTS	2,2´-azinobis 3-ethylbenzthiazolinesulfonic acid
amp	ampicillin
bp	base pair
DNA	desoyxy-ribonucleic acid
epPCR	error-prone PCR
FAD	flavin adenine dinucleotide
HRP	horseradish peroxidase
LB	Luria Bertani
PCR	polymerase chain reaction
P2Ox	pyranose 2 oxidase

Index

List of figures

List of tables

Summary

Pyranose 2 oxidase is a FAD dependent enzyme widespread in wood-degrading basidiomycetes. This enzyme has received increased attention as versatile biocatalyst in several biotechnical applications. The enzyme also has an important function in food industry due to the delivery of D-tagatose, which is a less-caloric, non-cariogenic sweetener with the same sweetness as sucrose.

The aim of this work was to elucidate the effects of various mutations in the active site of P2Ox on its catalytic activity and to improve the catalytic efficiency of the P2Ox in regard of its D-galactose conversion. This was approached by altering the enzyme with methods of site-directed mutagenesis (see PART 1) and directed evolution through error-prone PCR.

To enhance the catalytic efficiency of P2Ox derived from *Trametes multicolor* with the poor substrate D-galactose, error-prone PCR and site-directed mutagenesis were applied. The kinetic data of three mutants (H167A/T169G, N593S, 594del/t595K) were determined. The mutants did not exhibit improved catalytic constants with the substrate D-galactose.

Error-prone PCR and screening of 3000 mutants resulted in finding two improved variants over the P2Ox wild type enzyme. The determination of the standard enzyme activities of the mutants by a chromogenic ABTS assay was not part of this work and will be performed in another project.

1. Introduction

1.1 Pyranose 2-oxidase

Pyranose 2-oxidase (P2Ox; pyranose 2-oxidoreductase; glucose 2-oxidase; EC1.1.3.10) is a FAD dependent enzyme in wood degrading basidiomycetes and takes part in lignin degrading processes (21). Basidiomycetes are the only known microorganisms that are capable of fully mineralising lignin (15).

P2Ox is localized preferentially in the hyphal periplasmic space (6) of lignocellulolytic fungi. Only during autolysis P2Ox is located extracellularly and is associated with fungal cell walls or with extracellular slime (3, 7). The enzyme has a proposed role in lignocellulose degradation. P2Ox oxidizes aldopyranoses at position C2 to the corresponding ketoaldoses. The hydrogen peroxide (H_2O_2), which is produced during this reaction, is the essential co-substrate for two lignin-degrading oxidative enzymes, lignin peroxidase and manganese peroxidase (4, 5, 6).

P2Ox was purified and characterized from a number of microorganisms, like *Phanerochaete chrysosporium, Phlebiopsis gigantean, Pleurotus ostreatus, Polyporus obtusus* and *Trametes multicolor* (9, 17, 21). In this study P2Ox from *Trametes multicolor* was used (see Fig. 1).

Figure 11: *Trametes multicolor*

Pyranose 2-oxidase is a large, homotetrameric (see figure 2) flavoprotein with a molecular weight of approximately 270 kDa and consists of four identical 68 kDa subunits (18). A flavin adenine dinucleotid (FAD) acts as a cofactor and is covalently

bound to each of the four subunits at the N3 of the His167 residue via an 8α-methylic group. The FAD-cofactor is responsible for the yellow colour of the enzyme and shows typical absorption maxima at 456, 345 and 275 nm (13).

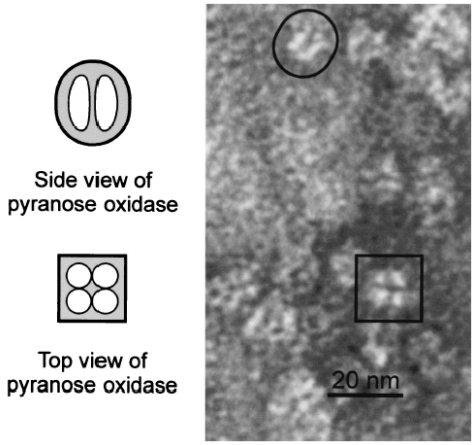

Figure 12: Transmission electron micrographs of P2Ox from *T. multicolor*

P2Ox catalyzes the regioselective oxidation of several aldopyranoses at the C2 position by molecular oxygen, forming the corresponding 2-ketoaldoses and H_2O_2 (6, 11). During the reductive half-reaction, the sugar is oxidized to the corresponding ketosugar and the co-factor FAD is reduced to $FADH_2$ (see equation a). The following oxidative half-reaction involves the reduction of O_2 to H_2O_2 and the regeneration of the co-factor (see equation b).

D-glucose + FAD → 2-keto-D-glucose + $FADH_2$ (a)

$FADH_2 + O_2 \rightarrow FAD + H_2O_2$ (b)

The in-vivo substrates of P2Ox are D-glucose, D-galactose, and D-xylose, which are abundant in lignocellulose and which are oxidized to 2-keto-D-glucose, 2-keto-D-galactose, and 2-keto-D-xylose, respectively. P2Ox also shows activity with other carbohydrates, like L-sorbose, D-glucono-1,5-lactone, and D-allose (10). In Table 1 the kinetic constants of P2Ox from *Trametes multicolor* with different sugar substrates and air saturation are shown. It is apparent, that D-glucose is the preferred substrate (18).

Table 6: Kinetic constants of P2Ox from *Trametes multicolor* with different sugar substrates and air saturation

substrate	K_m (mM)	k_{cat} (s^{-1})	k_{cat}/K_m (mM^{-1} s^{-1})	Relative activity (%)
D-glucose	0.74	54	73	100
5-thio-D-glucose	3.9	13	3.3	24
L-sorbose	38	53	1.4	99
D-xylose	30	30	1.0	56
D-glucono-1,5-lactone	38	34	0.91	64
D-allose	36	20	0.57	38
D-galactose	9.2	3.1	0.33	5.7
gentiobiose	62	12	0.19	23
D-mannoheptose	110	4.4	0.042	8.2
melibiose	120	4.6	0.038	8.6
L-arabinose	97	0.81	0.008	1.5

P2Ox also takes part in a secondary metabolic pathway by supplying 2-keto-D-glucose, which is the key intermediate leading to the antibiotic cortalcerone (1, 11).

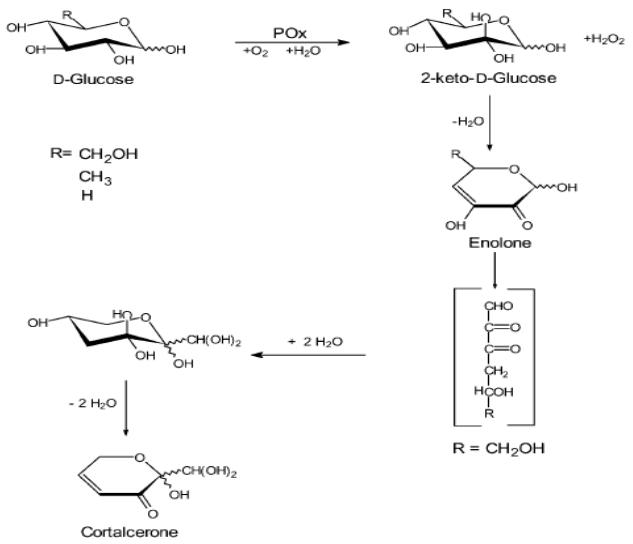

Figure 13: Biosynthesis pathway of antibiotic cortalcerone in white rot fungi

P2Ox can be used as key biocatalyst in several biotechnological applications and food industry. The oxidized 2-keto-sugars obtained from D-galactose and D-glucose can be reduced catalytically or enzymatically at position C1 to obtain high yields of virtually pure D-tagatose and D-fructose, respectively. To receive a decent amount of 2-keto-D-galactose it is necessary to improve the catalytic efficiency of the P2Ox regarding the conversion of D-galactose. The ketose sugar D-tagatose has a significant potential as a non-cariogenic, low caloric sweetener used in food applications (14).

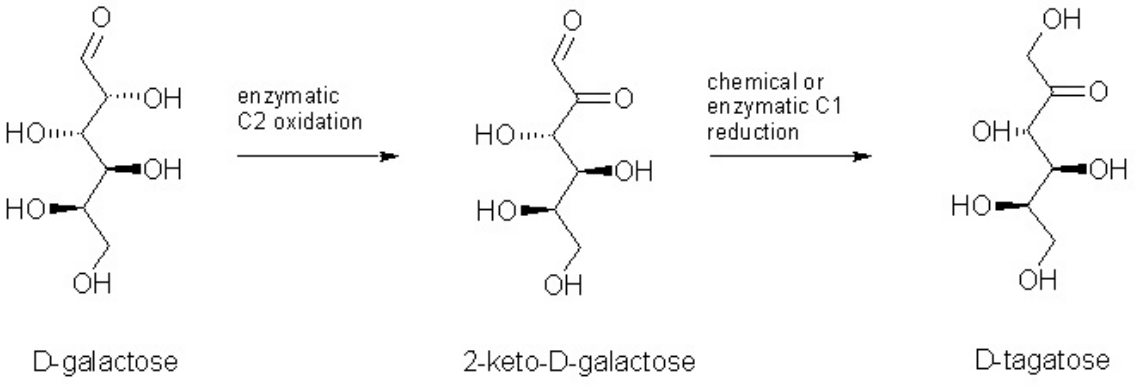

Figure 14: Synthesis of D-tagatose through C1 reduction of 2-keto-D-galactose

Applications of P2Ox in the field of bioprocess monitoring, clinical chemistry analytics and synthetic carbohydrate chemistry have been reviewed by Giffhorn (11). For example, it is used in clinical chemistry for determination of 1,5-anhydro-D-glucitol, an important marker for glycemic control in diabetes patients (11, 12).

1.2 Protein engineering

General

There are two general strategies for protein engineering, rational design and directed evolution. The rational design method uses detailed knowledge of the structure and function of the protein to make the desired changes. This method is inexpensive and easy, since site-directed mutagenesis methods are well-developed. It modifies a protein at specified locations of their amino acid sequence. A major drawback is that structural knowledge of a protein has to be available and it is difficult to predict the effects of the variations.
The second strategy is known as directed evolution (irrational design). Random mutagenesis is applied to a protein and a screening assay is used to pick out mutants that have the desired attributes. Further rounds of mutation and selection are then applied. This method mimics natural evolution. The advantage of directed evolution is that no knowledge of the protein structure is required.
The drawback is that they require high-throughput, which is not feasible for all proteins. Large amounts of colonies carrying the mutated DNA must be screened for desired qualities. Furthermore, not all desired activities can be easily screened for (19). The methods used to mutate the gene of interest are error-prone PCR and DNA shuffling. DNA-shuffling do not uses in contrast to the error-prone PCR method synthetic primers. Rational design and directed evolution techniques are amendatory. In this work the error-prone PCR was used.

Error prone PCR

Error-prone PCR is a mutagenesis technique to introduce randomized changes in the amino acid sequence in proteins. The mutations are introduced randomly during PCR

through the use of error-prone DNA polymerases and special PCR reaction conditions.

Because of its lacking proof-reading activity the Taq DNA-polymerase is used for error-prone PCR. The Taq polymerase has an error rate in the range of 0.1×10^{-4} to 2×10^{-4} per nucleotid per pass of the polymerase and lacks proofreading activity.

PCR reaction buffers containing $MnCl_2$ and dNTPs in unbalanced concentrations are added and the number of cycles is increased to achieve a useful mutation rate of 2-4 mutations per gene. The advantage of error-prone PCR is the ability to produce a lot of different mutated DNA strands. The drawback of this method is that a high number of colonies carrying these different mutated DNA strands have to be screened for the desired changes.

After epPCR, randomly mutated DNA sequences are ligated into an expression vector which is transformed into host cells and the resulting mutant libraries are screened for improved protein activity.

In this work epPCR was performed to alter the P2Ox encoding gene to find mutants with increased affinity to and improved catalytic activity with D-galactose. The mutants were screened by a (20).

2. Material

All present work was done at the Department of Food Sciences and Technology of the University of Natural Resources and Applied Life Sciences, Vienna, Austria.

Instruments

Sterile bench HS-P 12/2 (LF-Workbench) .....Heraeus
Labor autoclave, Certoklav EL, 10L/12L.....Kelomat
Autoclave, varioclave 500, 135L.....H+P Labortechnik
Centrifuge Sorvall RC 26 Plus.....Du Pont
Centrifuge Sorvall RC 5C .....Du Pont
Centrifuge Sorvall MC 12V .....Du Pont
Eppendorf Centrifuge 5415R.....INULA
UV/VIS Spectrophotometer Lambda2 .....Perkin Elmer

Diode Array Photometer Agilent 8453 .....Agilent technologies
pH-and conductivity electrodes.....WTW
Thermomixer compact.....Eppendorf
Thermocycler T3 Biometra .....Szabo Scandic
Plate reader SUNRISE .....Tecan Austria GmbH
Magellan software .....Tecan Austria GmbH
Gel Doc 2000 UV.....BIORAD Laboratories
SDS-PAGE Mighty small II .....Amersham Biosciences
Äkta .....Amersham Bioscience
Balances.....Sartorius analytic
Pipetes.....Eppendorf & Gilson

Molecular biology kits

Wizard SV Gel and PCR Clean-up system.....Promega
Wizard Plus Minipreps DNA Purification system .....Promega

Chemicals

All chemicals used were of the highest grade available and were purchased from Merck, Sigma and Fluka.

Media compounds were obtained from Sigma, Fluka, Carlo Erba, USB, Gibco BRL, Himedia, and BTS Biotechtrade Service GmbH.

Restriction enzymes, buffers and standards were purchased from Promega group, MBI Fermentas, SibEnzyme, BIO-RAD, and New England Biolabs.

Organisms

E. coli cells (BL21 DE3) were obtained from Invitrogen.

Media

LB_{Amp}-media	
Peptone	10 $g \cdot L^{-1}$
NaCl	10 $g \cdot L^{-1}$
Yeast extract	05 $g \cdot L^{-1}$
AMP	100 $mg \cdot L^{-1}$

LB_{Amp}-media + IPTG	
Peptone	10 $g \cdot L^{-1}$
NaCl	10 $g \cdot L^{-1}$
Yeast extract	5 $g \cdot L^{-1}$
AMP	100 $mg \cdot L^{-1}$
IPTG	0.5 mM

LB_{Amp}-agar	
Peptone	10 $g \cdot L^{-1}$
NaCl	10 $g \cdot L^{-1}$
Yeast extract	5 $g \cdot L^{-1}$
Agar	15 $g \cdot L^{-1}$
AMP	100 $mg \cdot L^{-1}$

TB_{Amp}-media	
Peptone	12 $g \cdot L^{-1}$
Yeast extract	24 $g \cdot L^{-1}$
Glycerine	4 $mL \cdot L^{-1}$
AMP	100 $mg \cdot L^{-1}$

Lactose-media	
D-Lactose	125 $g \cdot L^{-1}$

Media preparation

All media components were dissolved in deionized water and autoclaved at 121°C for 20 minutes. If ampicillin was added, the media was allowed to cool to at least 50°C before the addition of ampicillin.
Solid media (media for plates) was cooled down to approximately 50°C before it was poured into sterile petri dishes. Media plates were always prepared aseptically in a sterile bench. The plates were stored at 4°C until usage.
TB-media components were dissolved in 900 mL deionized water and autoclaved. Before usage 100 mL of a sterile KH_2PO_4-solution (0.17 M KH_2PO_4 / 0.72 M K_2HPO_4) were added aseptically.

Parental vector construct

The vector pHL2 was described by Kujawa et al. (16). The vector was derived from the expression vector pET21d$^+$ (Figure 5). It carries the P2Ox gene under the control of a T7 promoter obtained from *Trametes multicolor*.

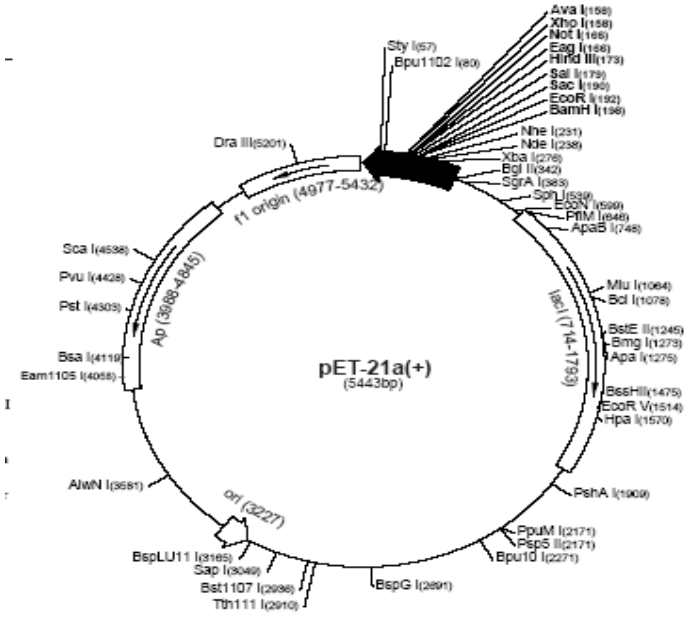

Figure 15: Restriction map of pET21d$^+$

pHL2 was derived from pET21d$^+$ by restriction with NcoI and NotI. The P2Ox gene was then ligated into the expression vector. The vector includes an ampicillin-resistance sequence, a *lacI* coding sequence, a T7 promoter, a multiple cloning site and a C-terminal His-tag.

3. Methods

3.1 site-directed mutagenesis

Generation of the mutants

The mutants H167A/T169G, 594del/T595K and N593S were created by Spadiut et al. in previous work. This work deals with the purification and kinetic characterization of these enzyme variants.

Biomass production

BL21 DE3 transformants were grown in TB_{amp} media in baffled shaking flasks (37°C, 160 rpm) to an OD_{600} of ~ 0.5. Protein expression was then induced by adding D-lactose to a final concentration of 0.5% (w/v) and cultures were further grown at 25°C and 140 rpm.
After 20 hours the biomass was harvested by centrifugation (6000 rpm, 30 min), diluted in the fourfold amount of KH_2PO_4 buffer (50 mM KPP, 20 mM Imidazole, 0.5 mM NaCl, pH 6.5) containing 0.1% PMSF (phenylmethylsulfonylfluorid) and lysed twice using the APV-2000 pressure homogenizer (Unna, Germany). The cells were separated from the crude extract by ultracentrifugation (30000 rpm, 30 min, 4°C) with a Beckman L70 Ultracentrifuge.

Protein purification

The supernatant was applied onto an IMAC (immobilized metal ion affinity chromatography) column. Utilising the binding effect of the pHL2 coded C-terminal His_6 groups with a Ni-sepharose gel, a His trap column (Amersham Biosciences) was used to purify the P2Ox mutants.
The supernatant was applied onto an IMAC (immobilized metal ion affinity chromatography) column. Utilising the binding effect of the pHL2 coded C-terminal His_6 groups with a Ni-sepharose gel, a His trap column (Amersham Biosciences) was used to purify the P2Ox mutants.
P2Ox was eluted with an elution buffer containing 50 mM KPP, 1 M imidazole,

0.5 mM NaCl (pH 6.5) with an imidazole gradient (0-100%, 60 mL, 3 $mL \cdot min^{-1}$) from 20 mM to 1 M.
The purified enzyme was washed with KH_2PO_4 buffer (50 mM KPP)**,** desalted and concentrated using Amicon® Ultra Centrifugal Filter Device (Millipore) with a cut off of 10 kDa to a final protein concentration of 5-10 $mg \cdot mL^{-1}$.

Protein concentration and activity measurements

Protein concentrations were determined by the Bradford assay (2). Bovine serum albumine (BSA) was used as standard.
The standard enzyme activities were measured with the chromogenic ABTS assay (8). 10 µl of the diluted enzyme were added to 990 µl of the reaction solution tempered to 30°C. The reaction solution contained 523.8 µg ABTS [2,2´-azinobis (3-ethylbenzthiazolinesulfonic acid], 142 Units horseradish peroxidase, KH_2PO_4 buffer (50 mM, pH 6.5) and either D-glucose (0.1-50 mM) or D-galactose (0.1-200 mM). The absorbance change at a wavelength of 420 nm was measured for 180 seconds. One unit P2Ox was defined as the amount of enzyme needed to oxidize 2 µmol of ABTS per minute. The chromophore ε_{420} used was 42.3 $mM^{-1}cm^{-1}$.

Additionally, the catalytic constants for 1,4-benzoquinone as electron acceptor were determined by adding 10 µl of diluted enzyme to 990 µl assay buffer containing either D-glucose or D-galactose (100 mM), KH_2PO buffer (50 mM, pH 6.5) and 1,4-benzoquinone in varying amounts (0.01–1.0 mM). The absorbance change at 290 nm was recorded at 30°C for 180 seconds. The chromophore ε_{290} used was 2.24 $mM^{-1}cm^{-1}$.

3.2 error prone PCR

Generation of mutants

As template the P2Ox gene containing two mutations (V546C and T169G) in its amino acid sequence was used. The used primers were T7fwd (3´- AATAC GACTCACTATAGGG -5´) and T7rev (3´- GCTAGTTATTGCTCAGCGG -5´).
The PCR mix was composed of the following components:

Table 7: Components of the epPCR mix

component	volume [µL]
H_2O	42
Taq puffer KCl (10x)	10
$MgCl_2$ (25 mM)	8
epdNTP mix (A/G: 30 mM, C/T: 10 mM)	10
template (plasmid V546C/T169G) (0.5 µg)	4
Taq DNA-polymerase (10 $U \cdot \mu L^{-1}$)	1
Primer T7 fwd (10 mM)	5
Primer T7 rev (10 mM)	5
$MnCl_2$ (3mM)	15
total volume	100

The PCR-Program was as follows:

Table 8: Program for the error prone PCR

temperature	duration	number of cycles
95°C	4 min	
94°C	30 sec	40 x
48°C	30 sec	
72°C	4 min	
72°C	10 min	
4°C	pause	

The PCR-product was applied on a 1% agarose gel and was run with 100 Volt.
The 2 kb bands were excised from the gel and the DNA was purified with the Wizard Gel & PCR Clean-Up System according the instructions.
Then the epPCR product and the template were cut at 37°C for 3 hours with the restriction enzymes NcoI/ NotI producing sticky ends.

Table 9: Components of the restriction of the plasmid V546C/T169G and the mutated epP2O DNA

component	volume [µL]
epP2O/ template (plasmid V546C/T169G)	30
10 x buffer O	5
Not I	2
NcoI I	4
H2O	9
total volume	50

After the restriction (4 h) the epPCR product and the backbone were loaded on a 1% agarose gel. The bands were excised according figure 6 and the DNA was purified with Wizard®SV Gel & PCR Clean-Up System.

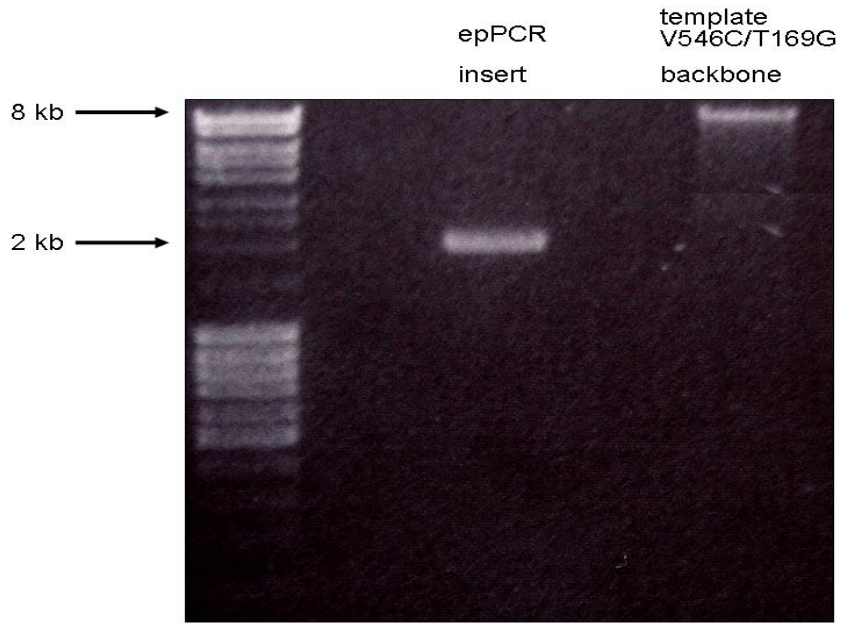

Figure 16: bands of epPCR product and backbone on an agarose-gel

Then the digested epPCR-product was ligated as insert to the backbone plasmid V546C/T169G using following ligation mix:

Table 10: Components of the ligation mix to ligate the insert in the backbone

component	volume [µL]
plasmid V546C/T169G (backbone)	15
epP2O (insert)	19
T4 DNA ligase buffer	4
T4 DNA ligase	2
totale volume	40

The PCR-program followed a temperature gradient from 10°C to 16°C with an elevation interval of 0.5°C every 30 minutes.

The ligation was purified, desalted and concentrated with Wizard®SV Gel & PCR Clean-Up System.

The mutated DNA was transformed into electrocompetent BL21 DE3 *E. coli* cells. After regeneration time of one hour at 37°C in the shaking incubator in SOC-Medium the cells were plated in aliquots on 4 LB_{Amp}-plates. The plates were incubated over night at 37°C.

Screening of the mutants

The mutants were screened with an ABTS enzyme activity assay in 96 well plates using D-galactose as substrate.

- The colonies of the mutant library growing on LB_{Amp}-plates were transferred with toothpicks in 96 wells plates containing 200 µL LB_{Amp}-Media. It was important just using single colonies.
- Six wells per master plate were inoculated with colonies carrying the mutations V546C/T169G to be able to compare the activity of the mutant enzyme with the activity of the wild type enzyme.
- Master plates were incubated over night at 25°C on a shaking incubator. (140 rpm)
- The working plates containing 200 µL LB_{Amp}+IPTG-Media were inoculated with the master plate cells using a replication stamp. The containing ITPG acted as inductor and induced protein expression.
- The working plates were also incubated over night shaking at 25°C.
- OD_{600} of each plate was measured to allow later comparison to normalize the values.
- The working plates were centrifuged at 3700 rpm for 5 min.
- The supernatant was discarded and the cell pellets were lysed by adding 100 µL Cell Lytic Buffer (Bugbuster) and incubating for one hour at room temperature on a shaker.
- Afterwards 100 µL KPP buffer (50 mM, pH 6.5) were added and the plates were centrifuged again at 3700 rpm for 15 minutes. The supernatant was used for the ABTS enzymatic activity screening assay.
- In new 96 well plates 80 µL of the ABTS reaction mix containing 0.035 $mg \cdot L^{-1}$ Horseradish peroxidase and 0.7 $mg \cdot mL^{-1}$ ABTS soluted in KH_2PO_4 (50 mM, pH 6.5) and 10 mL D-galactose (1 M) were added to each well.

- The reaction was started by adding 10 mL cleared supernatant of the working plates.
- The 96 well plates were incubated at 25°C.
- The absorption was measured at 420 nm. To receive standardized values the absorption values were divided by the corresponding OD_{600}.
- The average value of the wells containing the plasmid V546C/T169G was determined and compared to the values of the mutants.

3.3 Crystallography

At the KTH in Stockholm the crystal structures of the mutants H450G, F454P, Y456W, loop deletion and T169G/V546C/E542K were determined.
For the crystallization of the mutant enzymes the hanging-drop vapour diffusion method and micro seeding was used. Crystals of the recombinant proteins were obtained in the presence of 12-13% monomethyl ether PEG 2000, 50 mM $MgCl_2$ and 25% glycerol, 0.1 M 2-morpholinoethanesulfonic acid monohydrate (Mes) (pH 5.2) or 0.1 M Acetate (pH 4.6), respectively.
The enzyme solution and the crystallization buffer containing either Mes or Acetate both with and without Glycerol were applied in a drop on a thin plate. In each well of a 24-well plate the crystallization buffer was added and covered with the thin plate, the drop hanging downwards (see figure 7).

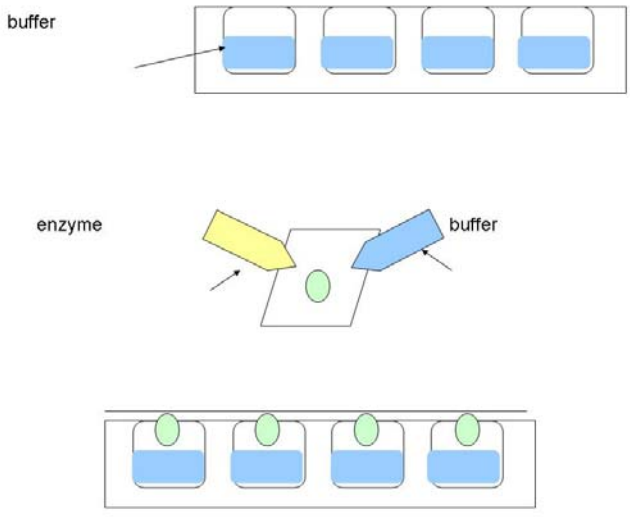

Figure 17: Scheme of the hanging drop method

In the covered wells arise a liquid-vapour-balance and the crystals begin to grow.
The crystal structure was determined with the synchrotron at the Max Laboratory in Lund by Prof. Divne.

4. Results

4.1 site-directed mutagenesis

The aim of this work was to elucidate the effects of various mutations in the active site of P2Ox on its catalytic activity and to improve the catalytic efficiency of the P2Ox in regard of its D-galactose conversion.

The kinetic values are shown in Tables 5-10.

- H167A/T169G

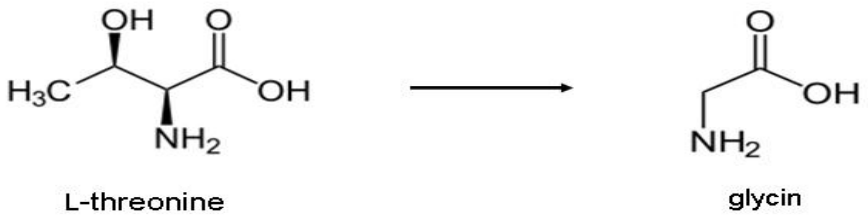

Figure 18: The replacement of the amino acid threonine at position 169 by glycine.

Threonine at position 169 localized in the active site of the enzyme was replaced with glycine. Glycine is the smallest amino acid and was expected to offer more space in the active site of the enzyme. Providing more space the substrate should enter more easily the active site and should bind better.

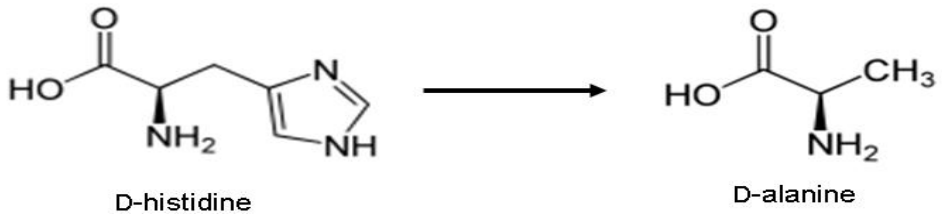

Figure 19: The replacement of the amino acid histidine at position 167 by alanine.

Histidine at position 167 was replaced with alanine. This mutation is also localized in the active site of the enzyme and was expected to offer more space for the substrate, due to the lacking imidazole circle of the histidine. FAD is tightly, but non-covalently bound. The replacement of threonine with glycine should offer more space for positioning of the FAD cofactor. The removal of the histidyl-FAD linkage resulted in former work in a catalytically worsened enzyme (16). The crystal structure of mutant His_6-H167A determined by Kujawa et al. (see figure 10) shows that the loop of the mutant enzyme is more opened compared to the wildtype enzyme to allow easy and fast entry of the substrates into the active site (16).

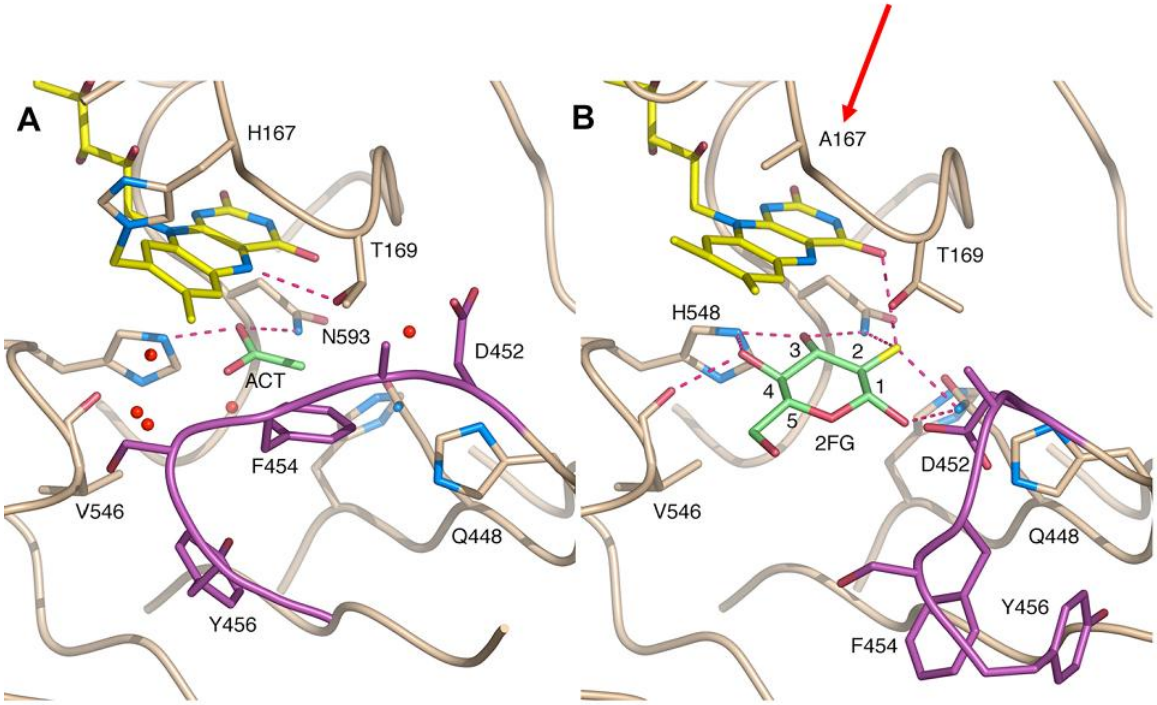

Figure 20: Crystal structure of the wildtype enzyme (A) and the mutant enzyme His-H167A (B).

Table 11: Kinetic data of the wildtype P2Ox and the mutant H167A/T169G with either D-glucose or D-galactose as sugar substrate and oxygen as electron acceptor (air saturation)

	D-glucose			D-galactose		
	K_M (mM)	k_{cat} (s^{-1})	k_{cat}/K_M ($mM^{-1}s^{-1}$)	K_M (mM)	k_{cat} (s^{-1})	k_{cat}/K_M ($mM^{-1}s^{-1}$)
wild type P2Ox	0.74	17.9	24.2	7.94	2.1	0.26
H167A/T169G	2.92	0.32	0.11	19.3	0.84	0.04

The mutant H167A/T169G showed with D-glucose as substrate and oxygen as electron acceptor a four times higher K_M value and a 50-times lower k_{cat} compared with wild type P2Ox. The resulting catalytic efficiency was 0.1 $mM^{-1}s^{-1}$. This meant a 240-fold decrease by comparison with the wildtype P2Ox.
Using D-galactose as substrate, the K_M value was three-fold increased and the k_{cat} was 2.5-times lower, resulting in a 6.5-times lower catalytic efficiency than the wildtype.

Table 12: Steady-State Kinetic Parameters for P2Ox enzymes measured for D-glucose as the electron donor

	D-glucose		
	K_M (mM)	k_{cat} (s^{-1})	k_{cat}/K_M ($mM^{-1}s^{-1}$)
wild type $P2Ox_a$	0.72	45.4	63.1
His_6-$H167A_a$	3.60	8.83	2.45
H167A/T169G	2.92	0.32	0.11

a) Kinetic data were determined in previous work by Kujawa et al. (16).

The introduction of the H167A/T169G mutation did not improve either the affinity of the mutant enzyme to the substrates or increased the turnover number of the substrates compared to the wildtype. By comparison with mutant His_6-H167A (see table 7) the K_M value was slightly decreased by the introduction of T169G, but the turnover number was even more decelerated.

Table 13: Kinetic data of the wildtype P2Ox and the mutant H167A/T169G with either D-glucose or D-galactose as sugar substrate and 1,4-benzoquinone as electron acceptor (sugar saturation)

	1,4-benzoquinone (D-glucose)			1,4-benzoquinone (D-galactose)		
	K_M (mM)	k_{cat} (s^{-1})	k_{cat}/K_M ($mM^{-1}s^{-1}$)	K_M (mM)	k_{cat} (s^{-1})	k_{cat}/K_M ($mM^{-1}s^{-1}$)
wild type P2Ox	0.40	348	862	0.25	6.61	26.3
H167A/T169G	0.10	1.35	13.0	0.2	3.23	16.3

With 1,4-benzoquinone as electron acceptor and either D-glucose or D-galactose as substrate the variant showed a 4-times and 2.5-times, respectively, decreased K_M value. Though the binding capability was improved, the reaction speed was decreased and was lower than that of the wild type enzyme. The k_{cat} value with D-glucose as substrate decreased for 350-times and the k_{cat} value with D-galactose was halved in contrast to the wildtype. This meant a 66-times lower catalytic efficiency using D-glucose and a halved catalytic efficiency using D-galactose as substrate.
Although the K_M of the mutant enzyme with 1,4-benzoquinone as electron acceptor because of the introduction of the mutation was improved, the turnover number decreased significantly, which resulted in a declined catalytic efficiency.

In former work the mutant His_6-H167A mutant was characterized by Kujawa et al. (16). This mutant displays significantly decreased k_{cat} value compared to that of the wild type when measured using saturating concentrations of D-glucose (>50mM) as substrate. Binding of substrate is affected to some degree in His_6-H167A as shown in table 7 by a five fold increase in K_M value.
By introduction of mutation T169G a mutant enzyme was expected displaying an improved binding capability of the substrates. The aim of mutation T169G was to offer because of the small amino acid glycine more space for the FAD cofactor to place and permit the substrates to enter and bind easy and fast the active site.
The kinetic data of the mutant enzyme H167A/T169G do not display the improvements expected of the mutations. For an increased turnover number it is

necessary that FAD is covalently bound, which is not given for the mutant H167A/T169G. The crystal structure of this mutant enzyme may give further reasons for these results.

- N593S

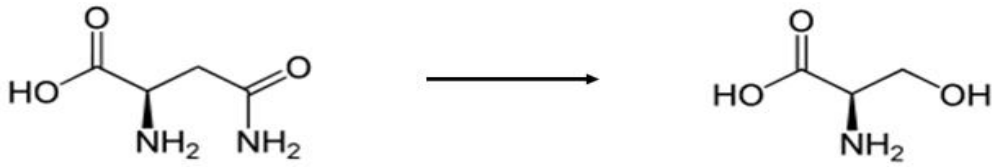

D-asparagine D-serine

Figure 21: The replacement of the amino acid asparagine at position 593 by serine.

Asparagine localized in the active site of the enzyme at position 593 was replaced by serine. The smaller amino acid serine is expected to offer more space for the sugar to bind at the active centre of the enzyme. The additional OH-group in the side chains of serine offers more binding possibilities for the substrates and resulting in the polar rejection the loop is expected to be more open and allow the substrates to enter faster. A lower K_M due to a better binding capability and a higher turnover number because of the faster substrate entry are expected.

Table 14: Kinetic data of the wildtype P2Ox and the mutant N593S with either D-glucose or D-galactose as sugar substrate and oxygen as electron acceptor (air saturation)

	D-glucose			D-galactose		
	K_M (mM)	k_{cat} (s^{-1})	k_{cat}/K_M ($mM^{-1}s^{-1}$)	K_M (mM)	k_{cat} (s^{-1})	k_{cat}/K_M ($mM^{-1}s^{-1}$)
wild type P2Ox	0.74	17.9	24.2	7.94	2.1	0.26
N593S	6.11	2.05	0.33	538	0.78	0.002

Mutant N593S showed an increased K_M value of 6.11 mM using the substrate D-glucose in the standard activity assay which meant a 9-fold rise compared to the wildtype. Compared to wild type P2Ox, the k_{cat} value decreased significantly to 2.05 s^{-1}. Concerning the catalytic efficiency, the mutant performed 75-times worse than wild type P2Ox.

With D-galactose as substrate and oxygen as electron acceptor the mutant N593S showed a 67-times higher K_M value and a 2.5-times lower k_{cat} value compared to wild type P2Ox, which results in a 260-times decreased catalytic efficiency.

The introduction of the mutation N593S did not result in an improvement of the catalytic efficiency converting D-galactose or D-glucose. The substrate may not benefit of the additional binding possibilities provided by serine. Reasons for the decreased k_{cat} value can be for example a not adequate loop opening of the mutant enzyme which was expected.

Table 15: Kinetic data of the wildtype P2Ox and the mutant N593S with either D-glucose or D-galactose as sugar substrate and 1,4-benzoquinone as electron acceptor (sugar saturation)

	1,4-benzoquinone (D-glucose)			1,4-benzoquinone (D-galactose)		
	K_M (mM)	k_{cat} (s^{-1})	k_{cat}/K_M ($mM^{-1}s^{-1}$)	K_M (mM)	k_{cat} (s^{-1})	k_{cat}/K_M ($mM^{-1}s^{-1}$)
wild type P2Ox	0.40	348.77	862.65	0.25	6.61	26.3
N593S	3.91	56.96	14.58	0.02	0.67	37.69

Using 1,4-benzoquinone as electron acceptor and D-glucose as substrate variant N593S showed a 10-times increased K_M value and a 7-times decreased value for k_{cat} compared to wild type P2Ox. Both the reaction speed and the binding capability of the mutant enzyme declined in comparison to the wildtype enzyme. The catalytic efficiency of the variant was 58-times lower by comparison with wild type P2Ox.

The K_M value for D-galactose as substrate with 1,4-benzoquinone as electron acceptor was 12-times lower compared with the wild type P2Ox. The turnover number for this substrate was 10-times decreased. The catalytic efficiency of variant

N593S with D-galactose as substrate and 1,4-benzoquinone as electron acceptor was slightly better than the catalytic efficiency of the wildtype.
The introduction of the mutation N593S improved the binding capability of the mutant enzyme towards 1,4-benzoquinone, but the reaction speed was decelerated. In summary, the mutation N593S improved slightly the catalytic efficiency using 1,4-benzoquinone as electron acceptor.

The reasons for the declined binding capability of the substrates can be that the sugar molecules do not reach the OH-groups provided by the introduced amino acid serine because of stereo chemic effects. It is possible that the intention to open the loop of the enzyme by polar rejection to allow easier and faster entry of the sugar molecules did not result in an adequate opening and the substrate can not enter the active site of the enzyme easier or faster.

- 594del/ T595K

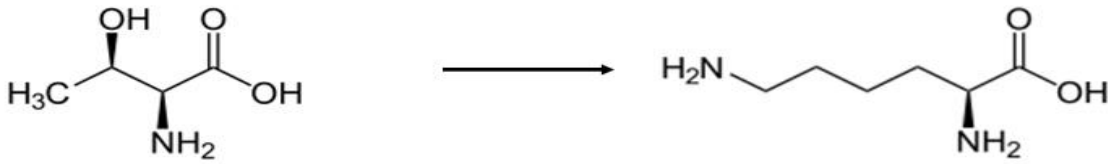

L-theronine L-lysine

Figure 22: The replacement of the amino acid threonine at position 595 by lysine.

The deletion of the amino acid close to the active site of the enzyme at position 594 offers more space for asparagine at position 593 to interact with the C4 of D-glucose. The enzyme is, due to the elevated flexibility, able to turn the sugar in the active site.
The introduced lysine instead of threonine at position 595 gained more space to deploy because of the deletion of the amino acid at position 595. It should be able to reach and bind due to the longer carbon side chain the sugar molecules entering the active site.

Table 16: Kinetic data of the wildtype P2Ox an the mutant 594del/T595K with either D-glucose or D-galactose as sugar substrate and oxygen as electron acceptor (air saturation)

	D-glucose			D-galactose		
	K_M (mM)	k_{cat} (s^{-1})	k_{cat}/K_M ($mM^{-1}s^{-1}$)	K_M (mM)	k_{cat} (s^{-1})	k_{cat}/K_M ($mM^{-1}s^{-1}$)
wild type P2Ox	0.74	17.9	24.2	7.94	2.1	0.26
594del/T595K	1.33	0.47	0.36	6.81	0.02	0.003

Using the substrate D-glucose in the standard activity assay, mutant 594del/T595K showed an increased K_M value of 1.33 mM, which meant a 50% increase compared to wild type P2Ox, and the k_{cat} value decreased significantly to 0.47 s^{-1}. Concerning the catalytic efficiency, the mutant performed 75-times worse than wild type P2Ox.

With D-galactose as substrate and oxygen as electron acceptor the K_M slightly reduced, but the turnover number was 100-times lower by comparison with the wildtype. The resulting catalytic efficiency of mutant 594del/T595K with D-galactose as substrate was also 75-times lower compared to the wildtype.

The mutant enzyme showed a slightly increased affinity towards D-galactose, but a decreased turnover number resulting in a declined catalytic efficiency.

An explanation for this can be that the introduced lysine binds the sugar molecules better than the replaced threonine. The asparagine at position 593 is because the deletion of the amino acid at position 594 potentially able for its full spreading and binds therefore the substrate molecules better. A reason for the declined reaction speed is maybe that the emerged space offered by the deletion of the amino acid at position 594 is used by the amino acids at position 593 and 595.

Table 17: Kinetic data of the mutant 594del/T595K with either D-glucose or D-galactose as sugar substrate and 1,4-benzoquinone as electron acceptor (sugar saturation)

	1,4-benzoquinone (D-glucose)			1,4-benzoquinone (D-galactose)		
	K_M (mM)	k_{cat} (s^{-1})	k_{cat}/K_M ($mM^{-1}s^{-1}$)	K_M (mM)	k_{cat} (s^{-1})	k_{cat}/K_M ($mM^{-1}s^{-1}$)
wild type P2Ox	0.4	348	862	0.25	6.61	26.3
594del/T595K	1.02	8.15	8.0	0.42	1.59	3.84

Using 1,4-benzoquinone as electron acceptor and D-glucose as substrate variant 594del/ T595K showed a doubled K_M value and a 40-times decreased value for k_{cat} compared to wild type P2Ox, resulting in a 107-times decreased catalytic efficiency.

The K_M value for D-galactose as substrate with 1,4-benzoquinone as electron acceptor was also doubled compared to wild type P2Ox. The turnover number for this substrate was decreased for four-times. The catalytic efficiency of variant V546C/E542K with D-galactose as substrate and 1,4-benzoquinone as electron acceptor was 6.8-fold lower than the catalytic efficiency of wild type P2Ox.

The deletion of the amino acid at position 594 and the introduction T595K did not improve the affinity of the mutant enzyme to the sugars nor accelerated the reaction speed.

In this case it is obvious that the introduced amino acid lysine do not bind the entering sugar molecules better than the replaced threonine. Also the additional space which is emerged by the deletion of the amino acid at position 594 does not allow the substrate molecules to enter the active site easier and faster.

4.2 error-prone PCR

To introduce additional mutation to improve the conversion of D-galactose we performed error-prone PCR. We introduced 1-2 mutations per P2Ox gene and screened libraries of 3000 colonies using a high-throughput screening assay.
The values of the measured absorption at 420 nm were standardized trough division by the corresponding OD_{600}. The average value of the wells containing the plasmid V546C/T169G was determined and compared to the values of the mutants.

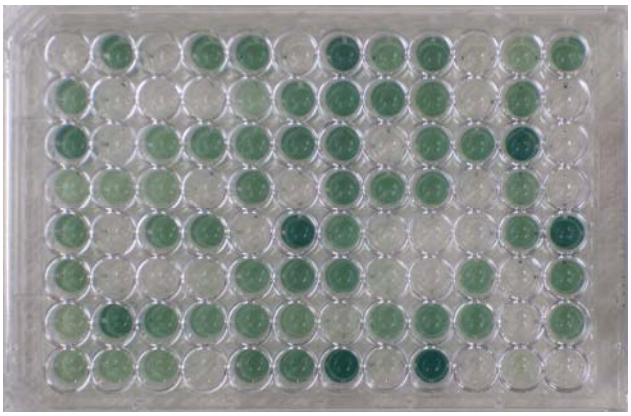

Figure 23: ABTS D-galactose screening in a 96-well plate

The colonies carrying a mutation, which improves the conversion of the D-galactose were picked together into a new 96 well plate and were screened again in a final screening assay with the substrate D-galactose. The mutants were compared once again with the plasmid V546C/T169G. The five best mutants were sequenced. The error-prone mutagenesis introduces following changes in the amino acid sequence, V546C/T169G + G387S/L560R and V546C/T169G + R466P. The residual three mutants did not exhibit mutations.

- V546C/T169G + G387S/L560R

Figure 24: The replacement of the amino acid glycine at position 387 by serine.

The mutation G387S is localized in the head of the enzyme and replaces the smallest amino acid glycine by serine. This may lead to a more flexible quaternary structure and the substrate enters the enzyme more easily. This mutation is expected to accelerate the reaction speed of the enzyme.

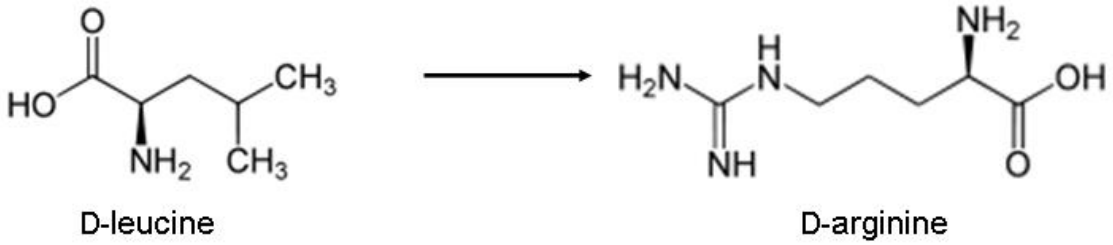

Figure 25: The replacement of the amino acid leucine at position 560 by arginine.

The mutation L560R is placed close the active site of the enzyme. The introduction of arginine instead of leucine enlarges because of the longer side chain the flexibility and therefore the ability of the amino acid to bind the sugar molecules. It is expected to lower the K_M value because of better binding of the sugar molecules.

- V546C/T169G + R466P

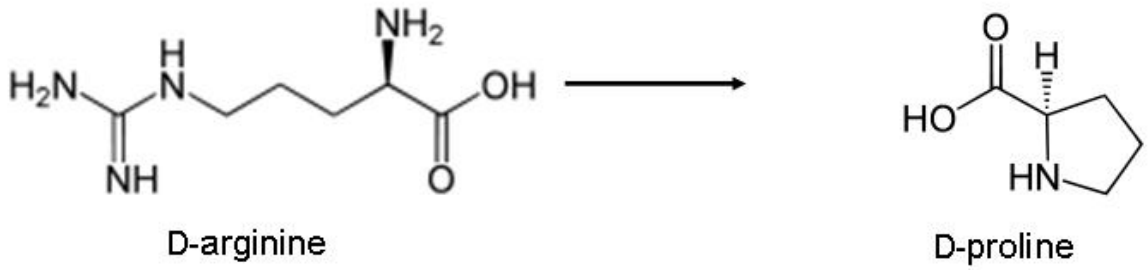

Figure 26: The replacement of the amino acid arginine at position 466 by proline.

The mutation R466P introduced by error-prone mutagenesis is positioned at the pivotal point of the enzyme. The amino acid proline replaces the bigger amino acid arginine. It is expected to keep the loop open due to polar rejection. The sugar molecules are able to enter the active site of the enzyme easier. This should increase the reaction speed of the enzyme.

The determination of the standard enzyme activities of the mutants by a chromogenic ABTS assay was not part of this work and will be performed in another project.

References

1. **Baute, M.-A., and R. Baute. 1984.** Occurrence among macrofungi of the bioconversion of glucosone to cortalcerone. Phytochemistry 2: 271-274.

2. **Bradford, M. M. 1976.** A Rapid and Sensitive Method for the Quantitation of Microgram Quantities of Protein Utilizing the Principle of Protein-Dye Binding. *Anal. Biochem.* 72: 248-254.

3. **Daniel, G. 1994.** Use of electron microscopy for aiding our understanding of wood biodegradation. FEMS Microbiol. Rev. 13: 199-233.

4. **Daniel, G., T. Nilsson, and B. Pettersson. 1989.** Intra- and extracellular localization of lignin peroxidase during degradation of solid wood and wood fragments by *Phanerochaete chrysosporium* by using transmission electron microscopy and immunogold labeling. Appl. Environ. Microbiol. 55: 871-881.

5. **Daniel, G., B. Pettersson, T. Nilsson, and J. Volc. 1990.** Use of immunogold cytochemistry to detect Mn(II)-dependent and lignin peroxidase in wood degraded by the white rot fungi *P. chrysosporium* and *Lentulina edodes*. Can. J. Bot. 68: 920-933.

6. **Daniel, G., J. Volc, and E. Kubatova. 1994.** Pyranose oxidase, a major source of H_2O_2 during wood degradation by *Phanerochaete chrysosporium*, *Trametes versicolor*, and *Oudemansiella mucida*. Appl. Environ. Microbiol. 60: 2524-2532.

7. **Daniel, G., J. Volc, E. Kubatova, and T. Nilsson. 1992.** Ultrastructural and immunocytochemical studies on the H_2O_2-producing enzyme pyranose oxidase in *Phanerochaete chrysosporium* grown under liquid culture conditions. Appl. Environ. Microbiol. 58: 3667-3676.

8. **Danneel, H.-J., E. Rössner, A. Zeeck, and F. Giffhorn. 1993.** Purification and characterization of a pyranose oxidase from the basidiomycete *Peniophora gigantea* and chemical analysis of its reaction products. *Eur. J. Biochem.* 214: 795–802.

9. **Danneel, H.-J., M. Ullrich, and F. Giffhorn. 1992.** Goal-oriented screening method for carbohydrate oxidases produced by filamentous fungi. Enzyme Microb. Technol. 14: 898-903.

10. **Freimund, S., A. Huwig, F. Giffhorn, and S. Köpper. 1998.** Rare keto-aldoses from enzymatic oxidation: substrates and oxidation products of pyranose 2-oxidase. Chem. Eur. J. 4: 2442-2455.

11. **Griffhorn, F. 2000.** Fungal pyranose oxidases: occurrence, properties and biotechnological applications in carbohydrate chemistry. Appl. Microbiol. Biotechnol. 54: 727-740.

12. **Griffhorn, F., S. Köpper, A. Huwig, and S. Freimund. 2000.** Rare sugars and sugar-based synthons by chemo-enzymatic synthesis. Enzyme Microb. Technol. 27: 734-742.

13. **Halada, P., C. Leitner, P. Sedmera, D. Haltrich, and J. Volc. 2003.** Identification of the covalent flavin adenine dinucleotide-binding region in pyranose 2-oxidase from Trametes multicolor. Analytical biochemistry. 314: 235-242.

14. **Haltrich, D., C. Leitner, W. Neuhauser, B. Nidetzky, K.D. Kulbe, and J. Volc. 1998.** A convenient enzymatic procedure for the production of aldose-free D-tagatose. Ann N Y Acad Sci. 1998 Dec 13: 864:295-9.

15. **ten Have, R., and P.J.M. Teunissen. 2001.** Oxidative mechanisms involved in lignin degradation by white-rot fungi. *Chemical Reviews* 101: 3397-3413.

16. **Kujawa, M., H. Ebner, C. Leitner, B. Hallberg, M. Prongjit, J. Sucharitakul, R. Ludwig, U. Rudsander, C. Peterbauer, P. Chaiyen, D. Haltrich, and C. Divne. 2006.** Structural Basis for Substrate Binding and Regioselective Oxidation of Monosaccharides at C3 by Pyranose 2-Oxidase. *J. Biol. Chem.* 46: 35104-35115.

17. **Leitner, C., D. Haltrich, B. Nidetzky, H. Prillinger, and K. D. Kulbe. 1998.** Production of a novel pyranose 2-oxidase by basidiomycete *Trametes multicolor*. Appl. Biochem. Biotechnol. 70-72: 237-248.

18. **Leitner, C., J. Volc, and D. Haltrich. 2001.** Purification and characterization of pyranose oxidase from the white rot fungus *Trametes multicolor*. *Appl. Environ. Microbiol.* 67: 3636–3644.

19. **Linda G. Otten, and Wim J. Quax. 2005.** Directed evolution: selecting today's biocatalysts. Biomolecular Engineering, Volume 22, Issues 1-3, June 2005, Pages 1-9.

20. **Spadiut, O., I. Pisanelli, T. Maischberger, C. Salaheddin, C. Peterbauer, L. Gorton, and D. Haltrich. 2007.** Engineering of pyranose 2-oxidase: improvement for biofuel cell and food applications through semi-rational protein design. Submitted to protein science.

21. **Volc, J., N. P. Denisova, F. Nerud, and V. Musílek. 1985.** Glucose-2-oxidase activity in mycelia cultures of basidiomycetes. Folia Microbiol. 30: 141-147.